TREND ANALYSIS OF THE DROUGHT OVER TURKEY

Master of Science Thesis

Rasha JAMAL

Eskisehir, 2019

TREND ANALYSIS OF THE DROUGHT
OVER TURKEY

Rasha Jamal

MASTER OF SCİENCE THESIS

HYDRAULICS/CIVIL ENGINEERING DEPT

Prof. Dr. Mustafa TOMBUL

Eskisehir

Anadolu University

Graduate School

May 2019

FINAL APPROVAL FOR THESIS

This thesis titled "TREND ANALYSIS OF THE DROUGHT OVER TURKEY" has been prepared and submitted by Rasha JAMAL in partial fulfillment of the requirements in "Anadolu University Directive on Graduate Education and Examination" for the Degree of Master of Science in Hydraulics Department has been examined and approved on 20.05.2019

Committee Members	**Title, Name and Surname**	**Signature**
Member (Supervisor)	Prof. Dr. Mustafa TOMBUL	
Member	Prof. Dr. Ali Savaş KOPARAL	
Member	Assoc. Prof. Dr. Hakan ŞİRİN	

Prof. Dr. Gürsoy Arslan

Director of Graduate School

ABSTRACT

TREND ANALYSIS OF THE DROUGHT OVER TURKEY

Rasha Jamal

Department of Civil Engineering

Programme in Hydraulics

Anadolu University, May 2019

Supervisor: Prof. Dr. Mustafa TOMBUL

Turkey was divided into 323 grids with 0.5º ×0.5º lat/lon. The Standardized precipitation evapotranspiration index (SPEI) values studied are for 1, 3, 6, and 12 months' time-scales for the periods of 1901-2015 / 1901-1981 / 1982-2015 were brought from http://spei.csic.es/, and the monthly Vegetation Condition Index (VCI) values were studied for the period of 1982-2015 and calculated depending on Normalized Difference Vegetation Index (NDVI) data brought from (AVHRR) sensors onboard (NOAA) satellite. The data for both SPEI and VCI were subjected to the Mann-Kendall's test to find out their trends, and their significance. Then the trend slope value was extracted by the Theil-Sen test. Finally, the Pettitt-Whitney test was used to find out the year of change in the trend. GIS software was used for the spatial trend analyzation. SPEI trend results suggested that drought trend prevails in most parts of Turkey with some variations when the time-scale changes from 1 to 12, however some parts such as northern, western, and some central parts of the country showed a wetter trend, with varying MKZ significance. However, unlike SPEI the VCI MKZ results ware significant for most of Turkey with not only less tendency to drought but tend to be a wetter trend. Such difference between SPEI and VCI analysis results can be attributed to the source of raw data used to obtain each index (SPEI is a meteorological-based index, while VCI is a satellite reflective-based index), that is why coincidence is not to be expected for those two indices.

Keywords: Drought, Turkey, Standardized precipitation evapotranspiration index, Standardized precipitation index, Vegetation Condition Index, Mann- Kendall's test, Theil- Sen's slope estimator, Pettit's test.

ÖZET

TÜRKİYE ÜZERİNDEKİ KURAKLIĞIN TREND ANALİZİ

Rasha JAMAL

İnşaat Mühendisliği Anabilim Dalı, Hidrolik Bilim Dalı

Anadolu Üniversitesi, Mayis 2019

Danışman: Prof. Dr. Mustafa TOMBUL

Türkiye, 0.5º × 0.5º eylem ve boylam olan 323 piksele (hücre) bölünmüştür. 1901-2015 /1901-1981 /1982-2015 dönemi ve 1, 3, 6 ve 12 aylık zaman ayarları için kullanılmış SPEI (Standardized precipitation evapotranspiration index) değerleri http://spei.csic.es/ 'den alınmıştır ve VCI (Monthly Vegetatiton Index, Aylık bitkisel indeksi) değerleri, 1982-2015 dönemi için çalışılmıştır ve (NOAA) uydudaki (AVHRR) sensorlardan alınan Normalleştirilmiş Fark Bitki Örtüsü İndeksi, 'NDVI' (Normalized Difference Vegetation Index) verilerine göre hesaplanmıştır. Hem SPEI hem de VCI için veriler, eğilimlerini ve önemini öğrenmek için Mann-Kendall testine tabi tutulmuştur. Ardından trend eğim değeri Theil-Sen testi kullanarak bulunmuştur. Ve trenddeki değişim yılını bulmak için Petit-Whithney testi kullanılmıştır. Mekânsal eğilim analizi için GIS (CBS) yazılımı kullanılmıştır. SPEI eğilim sonuçlarından, Türkiye'nin çoğu bölgesinde zaman ölçeğinin 1'den 12'ye değiştiği zaman biraz varyasyon ile kuraklık eğiliminin hüküm sürdüğünü önerilmiştir ve Türkiye'nin kuzey, batı ve bazı merkezi bölgeleri değişen bir MKZ önemi ile daha ıslak bir kuraklık eğilimi gösterilmiştir. Ancak, SPEI'den farklı olarak, VCI'nin MKZ sonuçları, yalnızca kuraklığa daha az meyilli değil aynı zamanda daha ıslak bir eğilimi olan Türkiye'nin çoğu için önemlidir. SPEI ve VCI analiz sonuçları arasındaki bu fark, her bir endeksi elde etmek için kullanılan ham veri kaynağına bağlanabilir (SPEI meteorolojik bazlı bir endeks iken VCI uydu yansıtıcı bazlı bir endekstir), bu nedenle bu endeksler arasında bir uyuşma beklenemez.

Anahtar Kelimeler: Kuraklık, Türkiye, Standardize yağış evapotranspirasyon endeksi, Standardize yağış endeksi, Bitki Örtüsü İndeksi, Mann-Kendall testi, Theil-Sen'in eğilim tahmincisi, Pettitt testi.

ACKNOWLEDGEMENT

First of all, I would like to express my special thanks to my thesis advisor, Prof. Dr. Mustafa Tombul for his invaluable guidance, and constant encouragement at all stages of the thesis.

I would like also to express my deepest gratitude to my supervisor Dr. Sinan Jasim Hadi for his patient guidance and precious advices throughout the research.

I must express my deep appreciation to my family, who has always been with me and supported me throughout my study.

I thank my friends J. Kanaan, Hanane, Nawal, Eyad, and Aziz for their positive support throughout the study.

Rasha JAMAL

20/05/2019

STATEMENT OF COMPLIANCE WITH ETHICAL PRINCIPLES AND RULES

I hereby truthfully declare that this thesis is an original work prepared by me; that I have behaved in accordance with the scientific ethical principles and rules throughout the stages of preparation, data collection, analysis and presentation of my work; that I have cited the sources of all the data and information that could be obtained within the scope of this study, and included these sources in the references section; and that this study has been scanned for plagiarism with "scientific plagiarism detection program" used by Anadolu University, and that "it does not have any plagiarism" whatsoever. I also declare that, if a case contrary to my declaration is detected in my work at any time, I hereby express my consent to all the ethical and legal consequences that are involved.

Rasha JAMAL

TABLE OF CONTENTS

LIST OF FIGURES

LIST OF TABLES

LIST OF ABBREVIATIONS

AE	: Aegean Regions.
AVHRR	:Advanced Very-High-Resolution Radiometer.
BS	: Black Sea Regions.
CA	: Central Anatolia Regions.
CDF	: cumulative distribution function.
Corine	: coordination of information on the environment.
DGA	: The Chilean Directorate General of Water.
EA	: eastern Anatolia Regions.
FAO	: Food and Agriculture Organization.
GIMMS	: Global Inventory Modeling and Mapping Studies.
GIS	: Geographic Information System.
MD	: Mediterranean Regions.
MK	: The Mann-Kendall test.
MR	: Marmar Regions.
MVC	: Maximum Value Composite NIR: Near-infrared.
NDVI	: Normalized Difference Vegetation Index.
NOAA	: National Oceanic and Atmospheric Administration.
PDF	: Probability density function
SEA	: southeastern Anatolia Regions.
SMCI	: Soil Moisture Condition Index.
SPEI	: Standardized precipitation evapotranspiration index.
SPI	: standard precipitation index.
TCI	: Temperature Condition Index.
WCRP	: World Climate Research Programme.
WMO	: World Meteorological Organization.

VegDRI : The Vegetation Drought Response Index

VCI : Vegetation Condition Index.

CHAPTER 1
INTRODUCTION

1.1. Introduction

Water cycle on planet Earth is responsible for evaporation, precipitation, transpiration, runoff, groundwater, etc. Environment and people depend on this cycle of water in nature to sustain environmental needs, human basic needs, agriculture, and economics. This cycle usually follows patterns depending on the region's location and topography. Drought is a disorder that effects these patterns as less precipitation than the usual takes place, causing shortage of water for all needs mentioned above. When drought occurs more frequent and for longer periods of time the water shortage turn into a serious problem, as all forms of life and human activities come under great stress. Drought became a more serious issue lately as it is occurring on more frequent, and severe basis that it became a great concern of researchers and decision makers. In an effort to understand and deal with drought, it was categorized into four types:

- Meteorological drought
- Agricultural drought
- Hydrological drought
- Socioeconomic drought

However, recently the term "Ecological drought" was introduced as well.

1.1.1. Drought definitions

Drought does not have a particular definition. It is usually defined according to its effects that are in focus. Precipitation is less than the statistical average for a region that causes water insufficiency for agricultural or economical activities, or for the environment. (NDMC, 2018c). Or it may be defined as follows: Drought is an extended period of less precipitation that causes a wide crop damages, or lowers its production (NDMC, 2018c). All climatic zones are vulnerable to drought no matter how high or low their average annual precipitation. Drought affects surface and ground water sources causing many troubles such as: loss of crops, loss of wet lands, an increase in forest fires, lower water supply, Health issues and transmigration of villagers to urban areas (NDMC, 2018b) .

Compared to other weather conditions - such as floods - drought is not an instantaneous effect phenomenon, since it takes a longer period of time to make an obvious impact. However, drought has long term effects that are severe, and widespread (Raleigh, Jordan, & Salehyan, 2008). Drought is a costly disaster as well, causing a lot of damages, losses, and mass migrations. For an example the cost of the four years drought of California was 2.7 billion dollars in the year 2015 (Doyle Rice, 2015). Drought also negatively affected hydro-electricity generation in Turkey which increases the cost of electricity production ("Kurak geçen kış elektrik fiyatlarında artışa neden olacak," 2018) (Poyraz, 2018).

1.1.2. Types of drought

-Meteorological drought: When precipitation becomes much lower than the long-term normal rate of a specific region. In time scale, this is the first step in drought occurrence (NDMC, 2018a). A continuous high-pressure weather system over a zone of land causes drought, where the weather is usually stable with clear skies. The normal circulation between dry and wet weather is then disrupted and drought occurs (Z. Sen, 29th July 2015).

- Hydrological drought: Usually it takes place after meteorological, it takes longer periods of drought occurrence to take place. It affects both surface (rivers, streams, reservoirs, etc.), and subsurface water supplies (NDMC, 2018a). When hydrological droughts occurs a remarkable decrease in groundwater, and stream flow is observed, in addition to a noticeable lower storage in dams and lakes, so hydrological drought affects all human activities in industrial, agricultural or urban areas(Z. Sen, 29th July 2015).

- Agricultural drought: Is when moisture in soil is not enough for the crops in the region as a result of meteorological drought. This takes place after both Meteorological and hydrological droughts (NDMC, 2018a).

- Socioeconomic drought: This occurs when water scarcity become harsh that it affects human activities in a way that it is unable to meet the human and environment demands, which affects economic and social activities of the society. This type usually follows the above mentioned types (NDMC, 2018a). Since human social and economic activities are deeply related to meteorological, industrial, and agricultural status, So when water supply-demand system is harmed by drought an important negative impact on socioeconomic status of people (Z. Sen, 29th July 2015).

- Ecological drought: A deficit in the normally available water supplies in a widespread manner for an extended period, which results in various stresses upon ecosystems — that includes alteration in both managed and natural hydrology — (NDMC, 2018a). (Figure 1.1) shows the succession of droughts occurrence, and their effects.

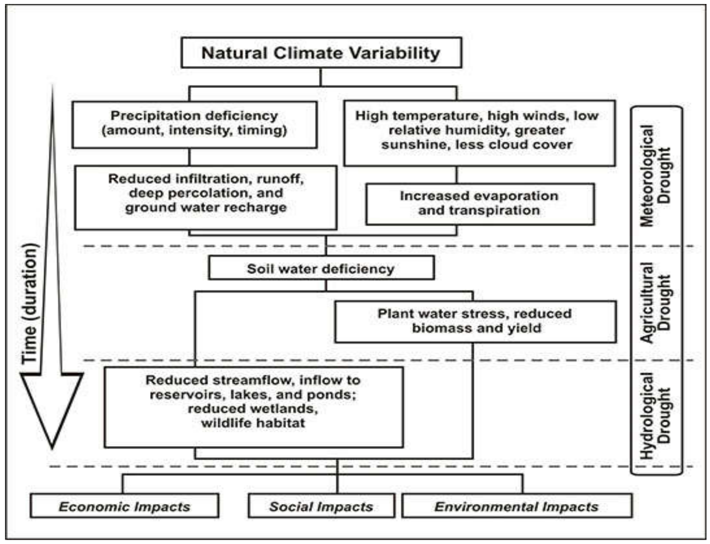

Figure 1.1. *succession of the occurrence of droughts and their effects (NDMC, 2018a)*

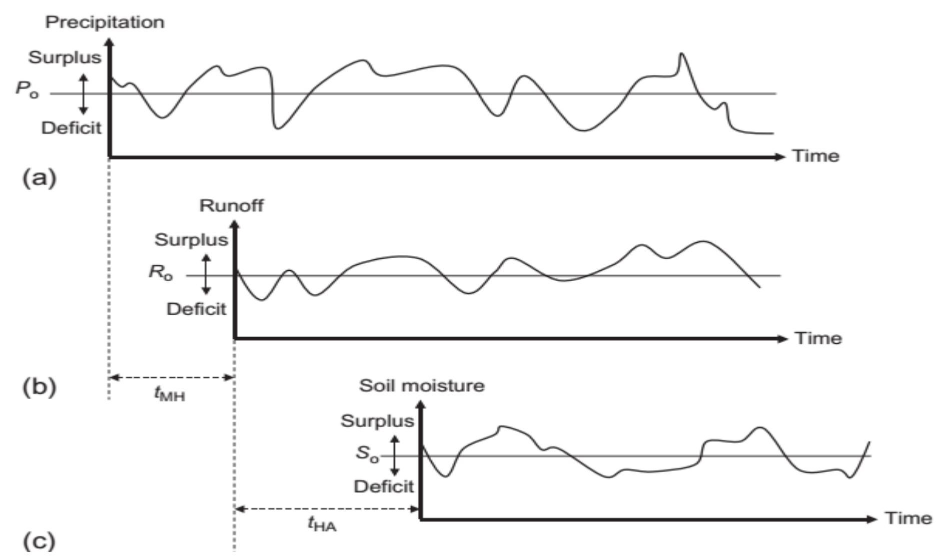

Figure 1.2. *Drought time lag: (a) meteorological, (b) hydrological, (c) agricultural (Z. Sen, 29th July 2015)*

t_{MH} is the time lag between the beginning of meteorological drought, and the beginning of hydrological drought which is essential for early warning and getting ready before water shortage and stress events take place. Similarly, t_{HA} is the time lag between the beginning of hydrological drought, and the beginning of agricultural drought which provides the necessary time to take precautions (Figure 1.2) (Z. Sen, 29th July 2015).

1.2. The Significance of the Study

The prime goal of the study is to investigate drought from 1901-2015 and comparing the periods before and after 1982 as well. The drought analysis were performed by determining the trend of two different drought indices which are, Standardized precipitation evapotranspiration index (SPEI), and Vegetation Condition Index (VCI). The SPEI values studied are for the time-scales of 1, 3, 6, and 12 months, for the 1901-2015 / 1901-1981 / 1982-2015 periods, while the VCI values were studied for the 1982-2015 period. The Mann−Kendall, and the Theil−Sen tests were applied on the Indices values to determine both the trend and its slope value to weigh the trend's extent. After that, the Pettitt test was applied to find out the 'most probable year of change' for the indices' trends. The trends were analyzed using the R statistical program, and the spatial patterns of the results were done by the GIS (Geographic Information System) software. Then the results were analyzed and discussed to explain the output trends.

1.3. Literature Review

Extensive researches have been done in different countries all over the world to analyze the drought using the drought index to detect the various drought types (Hydrological drought, Meteorological drought, ….etc.), while other researchers studied the trends of precipitation or temperature or both of them.

(Wang, Zhu, Xu, & Liu, 2015) investigated the drought intensity change in China. The drought intensity was researched depending on SPI, and SPEI indices, and using the Penman-Monteith equation to calculate evapotranspiration. The study used Monthly meteorological data from 633 sites in China for the period from 1961 to 2012. Modified Mann-Kendall test was used for trend detection in this study.

(Li, He, Quan, Liao, & Bai, 2015) This study was conducted in southwestern China. SPEI was applied to find out the drought patterns for the studied region for the years 1982-2012. The trend and severity of drought were determined depending on SPEI results. A comparison, and correlation of the results with SPI, VCI, and SMCI indices was done. The SPEI data was subjected to the (MK) test in order to determine the drought's trend, and the Mann-Kendall's "Z" values determined the trend's significance. The study concluded that the SPEI values were decreasing for (1,3,6,12, and 24 months) time-scale values, so a significant drying trend can be expected in the study area.

(Meza, 2013) In this paper, SPEI was used to conclude the drought trends of different extents to correlate them with the El Niño phenomenon, which is an atmospheric phenomenon of the oceans that affects the precipitation patterns in Northern parts of Chile. Daily precipitation data, and the max/min. temperatures for the stations that represent the study region were taken from The Chilean Directorate General of Water (DGA). The analysis focused on the 1970–2011 period, since the duration of record varied from one station to another, where some stations were recording since 1943, while other stations had only more recent period.

(Hernandez & Uddameri, 2014) Studied, and analyzed drought variability in semi-arid south Texas for (SPI), and (SPEI). They were related with precipitation and temperature projections which were taken from "Bias Corrected and Downscaled WCRP CMIP3 Climate Projections" for the 1950–2099 period. Three periods were considered in the study, a ‘‘historical’’ one covering from 1950 to 1999, an ‘‘early’’ one covering from 2000 to 2049, and a ‘‘late’’ period from 2050 to 2099.

(Sönmez, KÖmÜscÜ, Erkan, & Turgu, 2005) This study discussed the drought vulnerability of Turkey considering frequencies, occurrences, and regional distribution for the time-scales of 3, 6, 12, and 24-month. This study covered the period of 1951 to 2001 and analyzed the data of 101 meteorological stations. Using the Standard Precipitation Index (SPI), The study concluded that drought vulnerability had a steady form at different time-scales. It shows that southeastern and eastern parts suffer from mild droughts at short timescales (agricultural drought), while at the coastal part the droughts are mild but for longer durations (hydrological drought), although it can be noticed that coastal and interior tend to suffer severe droughts. It also concluded that regions that have a more wet weather are more affected by drought than less wet regions.

(Türkeş et al., 2016) This study investigated whether if the climate of Turkey is changing. The study depended on the data of 244 meteorological stations that included the temperature, and precipitation series for the 1950-2010 period. The data was subjected to several statistical methods (K-means, hierarchical clustering, Pitman-Morgan t-test, and paired t-test), these statistical tests helped to define precipitation patterns, and surface air temperature as well as providing a comparison to detect the change of meteorological trends for the two periods of (1950 – 1980) and (1981 – 2010). As a result; the study detects an increase of temperature after 1980, while precipitation patterns showed a considerable change after 1980 by an increase in the northern and eastern parts, and a decrease in the west, central and southern parts. This change was more obvious in the northern, eastern, central, central-east, and central-west Anatolia regions.

(Türkeş & Tatlı, 2009) Spatially and temporally analyzed the drought patterns in Turkey by using SPI values that were calculated for 40 stations, representing the different climatic regions in the country, presented by (Ağrı, Konya, Antalya, Trabzon, Göztepe, Şanlıurfa, Izmir) for the time-scales of 3-6-12-24 months during the 1940-1997 period.

(Hadi & Tombul, 2018) Studied the trend analysis of the long-term spatiotemporal for temperature, and precipitation all over Turkey using the monthly data obtained from (CRU TS V3.23) dataset for 81 grids during the period of 1901–2014. Trends were figured out by implementing the Mann−Kendall test, while the trend slope values were determined by using the Theil−Sen test. The Pettitt test was used after that to find out the 'most probable year of change' for both temperature and precipitation. The study concluded that the annual precipitation trend was significant depending on the Mann−Kendall test results, and the most frequent year of change was 1969, while the annual temperature also showed a significant and increasing trend all over Turkey, and the most probable year of change was 1993.

(Şorman, Mehr, & Hadi, 2018) Studied meteorological drought by analyzing SPEI and VCI. The study was for the period of 1982-2015. SPEI data were taken from (SPEI base v2.5) while VCI data was calculated depending on NDVI data from NOAA AVHRR, also land cover data was extracted from CORINE database.

(Sergio M Vicente-Serrano, 2007) applied VCI for the Iberian peninsula to detect the impact of drought on vegetation. He found out that VCI acts differently based on the climate, land cover, and the considered month. The study covered the period from 1987 to 2000. The study also used SPI. The study noticed that vegetation was affected in various ways depending on the location.

(Singh, Roy, & Kogan, 2003) used NDVI data from (AVHRR) of the (NOAA) to obtain VCI and TCI which were used to monitor the drought in India, and to assess the vegetation health. (Singh et al., 2003) also concluded that it is not enough to depend only on VCI to monitor the drought.

(Bhuiyan, Singh, & Kogan, 2006) the study was in Rajasthan province in India where an analysis was performed for meteorological and hydrological data for the years 1984-2003. The SPI and VCI indices were calculated, also the Standardized Water Level Index (SWI) was developed to estimate the deficit in groundwater recharge, it was found out that the relationship between VCI and SPI increases during the monsoon season because the health of plants depends entirely on rainfall, while partly controlled by irrigation during the rest of the year. the results showed an agreement with (Singh et al., 2003) that VCI is poorly correlated with other drought indices such as hydrological and meteorological.

1.4. Description of Thesis

The first chapter of the thesis includes brief information about drought, drought definition, and types. Previous studies were conducted in different countries all over the world to analyze drought by using drought indices were also mentioned in this chapter. In the second chapter details about the data used, and the study area, information and calculation method of (SPEI) and (VCI), term categories, and Drought categories of (SPEI) Values and (VCI) Values. Explanation of the methodology used in trend analysis for both (SPEI) and (VCI). Analysis results and discussion are presented in the third chapter. The last chapter provides the summary, conclusions and recommendations.

CHAPTER 2
DATA, STUDY AREA AND METHODS

2.1. Data and Study Area

2.1.1. Area of study

The research will cover all Turkey, Turkey is located between longitude 45-26 east and latitude 42-36 north in the subtropical region of the globe (Figure 2.1). Various regions of Turkey have dissimilar climates due to their uneven topography. Winter is responsible for most of the precipitation in Turkey, with an annual average precipitation ranging from 580 to 1300 mm in the Aegean and Mediterranean coasts, and 2200 mm in the eastern part of the black sea costs where it is the only part of Turkey that rains all around the year (Sensoy, Demircan, Ulupinar, & Balta, 2008). The mean temperature in Central Anatolia ranges from 8 to 12C°, while it ranges from 12 to 16C° in the coastal areas of Black Sea, Marmara, central part of the Aegean Sea and the Mediterranean inland, and it ranges from 16 to 20 C° in the Aegean and Mediterranean coastal areas, and all part of southeastern Anatolia (Sensoy, 2004).

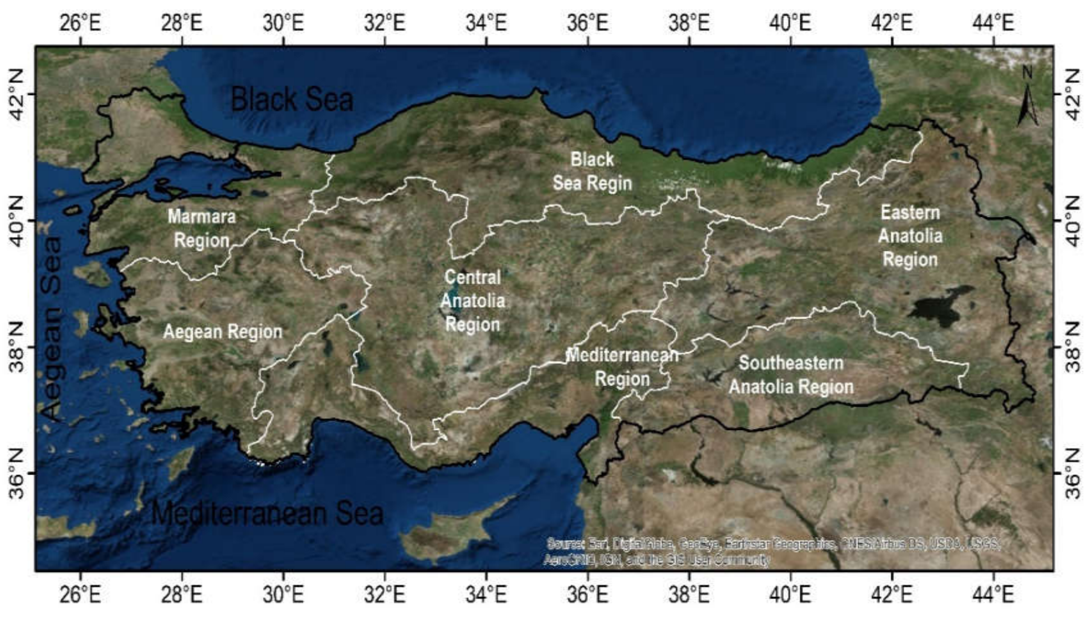

Figure 2.1. *Regions of Turkey: Black Sea (BS), eastern Anatolia (EA,) southeastern Anatolia (SEA), Central Anatolia (CA), Mediterranean (MD), Aegean (AE), Marmara (MA)*

2.1.2. Used data

2.1.2.1. Data of SPEI

SPEI base is a Global SPEI database that contains long-time information of drought indices of the world. The data has a spatial resolution of 0.5º lat/lon. A multiple scale SPEI values of (1, 3, 6, 12, and 48) months is provided. The data is available for the period from January 1901 up to December 2015. In this study SPEI version 2.5 is used (obtainable at http://spei.csic.es/) with the Spatial resolution mentioned above (Sergio M. Vicente-Serrano). The potential evapotranspiration is calculated using The FAO-56 Penman-Monteith equation (R. G. Allen, Pereira, Raes, & Smith, 1998). According to all that, there are 323 pixels (size 0.5 degrees × 0.5 degrees) distributed over the entire area of Turkey. Every pixel has SPEI values for the period of 1901-2015, for (1, 3, 6, 12 months) time-scales. Each pixel was represented by a central point located in the center of it to facilitate the study (Figure 2.2) shows the distribution of points all over Turkey.

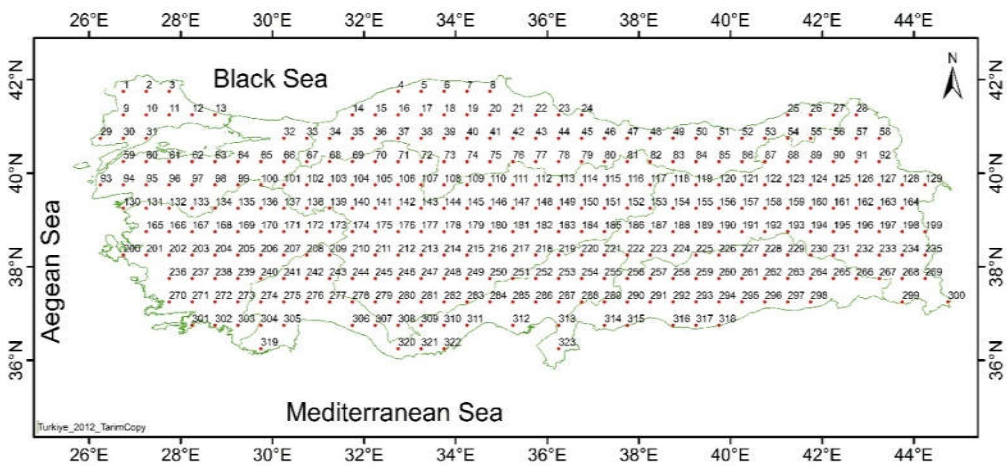

Figure 2.2. *The distribution of points all over turkey*

2.1.2.2. Data of VCI

Vegetation indices are obtained by using the radar to measure the absorbed radiation by the green parts of the plants to figure out the functioning greenness of the surface on the level of a region (CimateDataGuide, 2018). NDVI 3rd generation values are used to calculate VCI depending on the Global Inventory Modeling and Mapping Studies (GIMMS) project. The (AVHRR) sensors of the (NOAA) satellite provide the needed GIMMS NDVI values. This study uses version 3g.v1.0 and involves the period from July-1981 to December- 2015. These data are time-scaled on biweekly basis with a resolution of 8 km. In order to obtain a monthly scale so that it can be compared with SPEI, MVC (the Maximum Value Composite) method is used were the maximum value is taken to make sure that the deleterious effects such as aerosols and clouds are minimized (Şorman et al., 2018; Tucker et al., 2005) +the VCI values for Turkey in this study start from January-1982 because the monthly data of the year of 1981 are not complete, so it was removed.

Using R statistical program; a Raster resample was done so that the spatial resolution of both VCI and SPEI can be matched with each other.

2.2. Drought Indices

2.2.1. Standardized precipitation index (SPI)

Developing indices to monitor drought was a main interest for scientists and experts in the field of meteorology (appendix /1/ shows drought indices development with time)(Heim Jr, 2002). In 1993 the Colorado State University developed the SPI drought index (Standardized Precipitation Index). This index represents a probability value that can describe the drought status regardless of climate, location, or time period (Z. Sen, 29th July 2015). SPI is the difference between the mean and recorded precipitation for a given period of time divided by the standard deviation, where past records are the source of both the mean precipitation and the standard deviation. (McKee, Doesken, & Kleist, 1993)

$$P_i = \frac{P_i - \bar{P}}{S_p} \tag{2.1}$$

Where P_i is the precipitation at the time i, P is the long term average, S_p standard deviation (Z. Sen, 29th July 2015).

- SPI calculation method

- A monthly series of precipitation data for m months is collected, and it is preferred if these data were continuous for 30 years at least.

- A set of averaged periods are prepared to produce a time-scale for a period j (j is 3, 6, 12, 24, or 48 months), (these time-scales are representative of precipitation deficits for the different types of drought related to different water uses and resources).

- The data set is moving in the sense that each month a new value is determined from the previous i months. Each of the sets are fitted to the Gamma function to find out the probability to precipitation relationship.

- After the probability to precipitation is found then the probability of any precipitation data point is calculated. The resulting probabilities are then used along with the inverse normal to specify the deviation of the precipitation for a normally distributed probability density, this deviation is the SPI at this precipitation data point (McKee et al., 1993) .

- SPI values have several term categories with respect to the term of the time they are applied to, as shown below

1) **1-month SPI:** reflects the short-term meteorological form of drought. This one concerns short-term issues such as soil moisture, plants stress, particularly for crop growing seasons.(WMO, 2012)
2) **3-month SPI:** This time-scale is a procedure that enables the comparison between the precipitations for any given period of 3 months with the same 3-months periods for all the years of the historical record. This time-scale is the reflection of the moisture conditions for short-term and medium-term, a seasonal estimation of precipitation in primary agricultural regions can be provided by this scale as well. (WMO, 2012)
3) **6-month SPI:** Same as in SPI-3, the comparison here is between 6-month periods instead of 3. (WMO, 2012)
4) **9-month SPI:** This one stretches into the medium time-scale periods, which is an indication for inter-seasonal precipitation trends. When the SPI value for this time-scale is less than 1.5 then an important negative impact can be expected on agriculture due to dry conditions, which may extend to other activities. (WMO, 2012)
5) **12-month and 24-month SPI:** These time-scales are generally linked to stream flows, reservoir levels, and to groundwater levels at longer time-scales. (WMO, 2012)

(Thom, 1958) mentioned that the most suitable PDF (probability distribution function) for precipitation records is the Gamma PDF (Z. Sen, 29th July 2015). This PDF has only positive x values and calculated as:

$$f(x) = \frac{1}{\beta^{\alpha}\Gamma(\alpha)} x^{\alpha-1} e^{-x/\beta} \tag{2.2}$$

Where x the value of the rain to which the distribution is to be evaluated α, β are shape and scale parameters. They have a value greater than zero $\Gamma(\boldsymbol{\alpha})$ is the Gamma function defined by

$$\Gamma(\boldsymbol{\alpha}) = \int_{\mathbf{0}}^{n} \boldsymbol{y}^{\boldsymbol{\alpha}-\mathbf{1}}\, \boldsymbol{e}^{-\boldsymbol{y}}\mathrm{dy} \tag{2.3}$$

$$\hat{\alpha} = \frac{1}{4A}(1 + \sqrt{1 + \frac{4A}{3}}) \tag{2.4}$$

$$\hat{\beta} = \frac{\bar{x}}{\hat{\alpha}} \tag{2.5}$$

$$A = \ln(\bar{x}) - \frac{\sum \ln(x)}{n} \tag{2.6}$$

Where n is the number of precipitations

When the parameters for a specific time-scale are calculated, they are used to find out CDF (Cumulative Distribution Function) of precipitation:

$$G(x) = \int_0^x g(x)\mathrm{dx} = \frac{1}{\hat{\beta}^{\hat{\alpha}}\Gamma(\hat{\alpha})} \int_0^x x^{\hat{\alpha}-1} e^{-1/\hat{\beta}}\, \mathrm{dt} \tag{2.7}$$

or t = x/β transformation leads to

$$G(x) = \frac{1}{\Gamma(\hat{\alpha})} \int_0^x t^{\hat{\alpha}}\, e^{-1}\mathrm{dt} \tag{2.8}$$

(Thom, 1958) provided a table that contains incomplete Gamma PDF, and G(x) values. This function is unknown for any x. In addition, any precipitation distribution includes zero values; in this case, the CDF is expressed as:

$$H(x) = q + (1 - q)G(x) \tag{2.9}$$

Where, q is the probability of precipitation less duration. For a sequence of length n, with m zero precipitation number then the calculation is:

$$q = \frac{m}{n} \tag{2.10}$$

The CDF, H(x), with its arithmetic average equal to 0 and variance 1, is converted to standard normal (Gaussian) CDF, Z-score, which are known as the SPI values. Panofsky and Brier (1958) have offered a method to convert any PDF, to a standard normal PDF (Figure 2.3).

$$Z = SPI = -\left(t - \frac{2.515517 + 0.802853t + 0.010328t^2}{1 + 1.432788t + 0.189269t^2 + 0.001308t^3}\right) \text{ for } 0<H(x)\leq 0.05 \quad (2.11)$$

$$Z = SPI = +\left(t - \frac{2.515517 + 0.802853t + 0.010328t^2}{1 + 1.432788t + 0.189269t^2 + 0.001308t^3}\right) \text{ for } 0.5<H(x) <1 \quad (2.12)$$

$$\boldsymbol{t} = \sqrt{\boldsymbol{ln}\left(\frac{\mathbf{1}}{(\boldsymbol{H}(\boldsymbol{x}))^{\mathbf{2}}}\right)} \quad \text{for } 0<H(x)\leq 0.05 \quad (2.13)$$

$$\boldsymbol{t} = \sqrt{\boldsymbol{ln}\left(\frac{\mathbf{1}}{\mathbf{1}-(\boldsymbol{H}(\boldsymbol{x}))^{\mathbf{2}}}\right)} \quad \text{for } 0.5<H(x) <1 \quad (2.14)$$

Scientist (McKee et al., 1993) has classified SPI values into eight categories that describes the precipitation status ranging from dry to wet (Table 2.1).

Table 2.1. *SPI Values and Drought Category.*

SPI Values	Drought Category
≥2	Extremely wet
1.50 to 1.99	Severely wet
1 to 1.49	Moderately wet
0 to 0.99	Mild wet
-0.99 to 0	Mild drought
-1.49 to -1	Moderate drought
-1.99 to -1.5	Severe drought
≤-2.00	Extreme drought

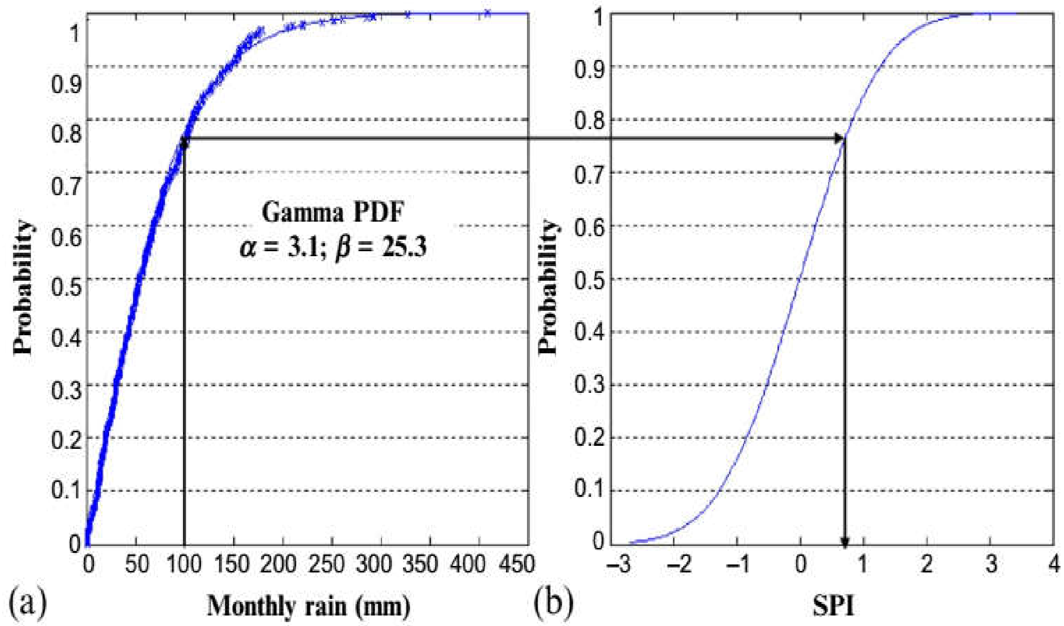

Figure 2.3. *Example of an equiprobability transformation from a fitted gamma distribution to the standard normal distribution(Z. Sen, 29th July 2015)*

2.2.2. Standardized precipitation evapotranspiration index (SPEI)

For a while SPI prevailed as the most dependable drought index, but since the global temperature rose significantly in the last 100 years a new index (SPEI) was developed so that to take temperature into consideration rather than just precipitation as in the case of (SPI), which made it a stronger index. Unlike (SPI), (SPEI) needs complete data. SPEI uses monthly precipitation and temperature data (WMO, 2016). In the year 2010 SPEI (standard precipitation evaporation index) was introduced; and thereafter was used to perform many climate and hydrological studies. (Beguería, Vicente-Serrano, Reig, & Latorre, 2014) Such studies that analyzed drought variability (Potop, 2011), drought reconstruction (K. Allen, Ogden, Buckley, Cook, & Baker, 2011), climate change (Abiodun, Salami, Matthew, & Odedokun, 2013), ecological systems (Martin-Benito, Beeckman, & Cañellas, 2013), Many studies that used SPEI have noted that SPEI is more associated with ecological and hydrological parameters than other drought indices. (Beguería et al., 2014) The processes used to calculate the SPEI are similar to those used to calculate the SPI, but the SPEI has a balance that offset the difference between precipitation and evaporation instead of using only the precipitation as an input (Sergio M. Vicente-Serrano).

$$D_i = P_i - PET_i \tag{2.15}$$

Where D_i is the water of that month, P_i the precipitation of a given month, and PET_i the potential evapotranspiration for that month (Sergio M. Vicente-Serrano).

The climatic water balance series is done based on different time-scales (Beguería et al., 2014). It is hard to choose the statistical distribution that best suits the D series pattern (Sergio M. Vicente-Serrano). According to (BEGUERíA, Vicente-Serrano, & Angulo-Martínez, 2010; Beguería et al., 2014; Sergio M. Vicente-Serrano) the log-logistic distribution leads to better results than other distributions and it is more suitable for the resulting values to convert the original values into standardized units that can be compared in place and time for various SPEI time-scales (Sergio M. Vicente-Serrano):

$$f(x) = \frac{\beta}{\alpha}\left(\frac{x-\lambda}{\alpha}\right)\left[1+\left(\frac{x-\lambda}{\alpha}\right)\right]^2 \tag{2.16}$$

The probability distribution function of a variable D according to a log-logistic distribution is given by:

$$\mathrm{F(D)} = \left[1+\left(\frac{\alpha}{D-\gamma}\right)^{\beta}\quad\right]^{-1} \tag{2.17}$$

Where $\boldsymbol{\alpha}$, $\boldsymbol{\beta}$ and γ are the scale, shape, center parameters D value must be within the limited range ($\gamma < D < \infty$) (Sergio M. Vicente-Serrano). (Hamed & Rao, 2000) originally, suggested the use of PWMs (Probability Weighted Moments) by depending on plotting position method. Various orders of PWMs are obtained as follows:

$$w_s = \frac{1}{N}\sum_{i=1}^{N}(1-F_i)^s D_i \tag{2.18}$$

Where, w_s is the PWM of order s, N is the number of data points, F_i is a frequency estimator, and D_i is the difference between Precipitation and Reference Evapotranspiration for month i. However there are other ways to calculate PWM estimators, unbiased estimator for example (Hosking, 1986).

$$w_s = \frac{1}{N}\sum_{i=1}^{N}\frac{\left(\frac{N-i}{s}\right)D_i}{\left(\frac{N-1}{S}\right)} \tag{2.19}$$

Even though SPEI used to be based on PWM (Plotting-positions Probability Weighted Moment), it is recommended to use unbiased PWM for model fitting is recommended (Beguería et al., 2014). With F(D) the SPEI can be obtained as the standardized values of F(D).

$$SPEI = W - \frac{C_0 + C_1 W + C_2 W^2}{1 + d_1 W + d_2 w^2 + d_3 w^3} \tag{2.20}$$

Where $W = -\ln(P)$

For P ≤ 0.5, P=1-F(D) is the probability of exceedance of a specific D value. For P≥0.5, P value is replaced by 1-P and the SPEI value is inverted. The constants are: C_0 = 2.515517, C_1= 0.802853, C_2 = 0.010328, d_1=1.432788, d_2 = 0.189269, d_3 = 0.001308 (Beguería et al., 2014; Şorman et al., 2018; Sergio M. Vicente-Serrano). The average value of the obtaining SPEI is 0, and the standard deviation is 1 (Beguería et al., 2014; Sergio M Vicente-Serrano, Beguería, & López-Moreno, 2010).

There are many equations that can be implemented to model PET using available data (e.g. the Hargreaves equation, the Penman-Monteith equation, the Thornthwaite equation, etc.), taking into account that SPEI is not tied to any specific equation. Now the FAO-56 Penman–Monteith equation is used to calculate SPEI replacing the Thornthwaite equation (Thornthwaite, 1948) which was used earlier (R. G. Allen et al., 1998) was used to calculate SPEI base v2.0.

2.2.3. Normalized difference vegetation index (NDVI)

It is an index of the agriculture drought. It uses the global vegetation index data provided by NOAA, AVHRR satellite (where the Radiance values; are measured in the visible and near-infrared channels). NDVI was vastly used in the last 2 decades to monitor agricultural drought (Sivakumar et al., 2011). Green vegetation covers the red and near infrared zone of the spectral reflection, it is calculated as follows:

$$NDVI = \frac{\text{Near infrared band} - \text{Rad band}}{\text{Near infrared band} + \text{Rad band}} \tag{2.21}$$

Where (Near infrared band + Rad band) removes the effects of different sun and view angles (Sunar Filiz, 2011). NDVI values are theoretically between (-1 and +1). However, usually most spotted NDVI values on Earth ranges from near 0.0 for bare surfaces to about 0.9 for densely vegetated areas (Sivakumar et al., 2011). In area where there is more green vegetation the value of NDVI becomes close to +1 while for rock areas and arid soil the value of NDVI become close to 0 because reflective features are similar in Red and near infrared region, and it becomes closer to -1 for snow and clouds. NDVI values are higher when green vegetation increases; if the plant cover is under stress and chlorophyll production is reduced and the color will appear more yellow as there will be more reflection in the Red zone which will result in a lesser amount of near infrared (Sunar Filiz, 2011) (Figure 2.4).

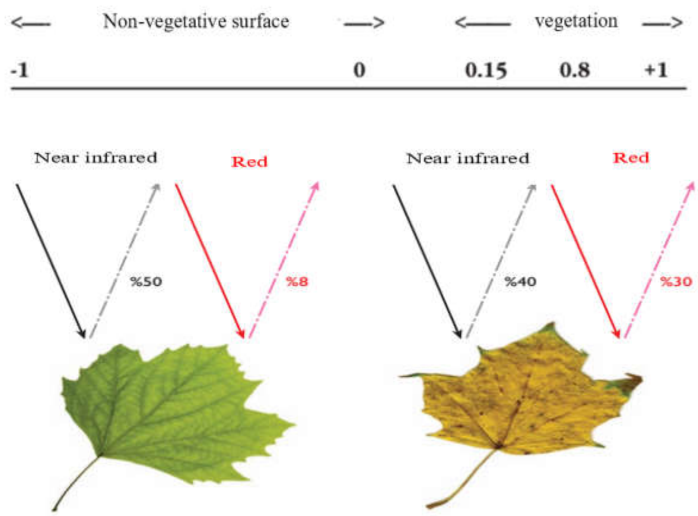

Figure 2.4. *Values of NDVI for different leaf reflectors(Sunar Filiz, 2011)*

The plant growth rate index (NDVI) was widely used in many studies such as plant monitoring, estimation of crop production, and the detection of drought (Benedetti & Rossini, 1993), the analysis of agricultural drought (Sruthi & Aslam, 2015). Since most satellites are equipped to detect red and NIR bands, NDVI can be easily calculated using the data of these many satellites (Sivakumar et al., 2011).

2.2.4. Vegetation condition index (VCI)

Usually used with (NDVI), however (VCI) gives results that are more accurate. It uses AVHRR satellite thermal bands data. VCI It is better than NDVI as an indicator for the water stress condition monitoring (Kogan 1995). The quality of VCI depends mainly on the quality of NDVI since it is derived from NDVI, as well as the length of the historical time series available at (CGLS). VCI results have better accuracy than NDVI in the regional scale (Bajgiran, Darvishsefat, Khalili, & Makhdoum, 2008).

VCI is calculated as follows:

$$VCI = 100 * (\frac{NDVI_i - NDVI_{min}}{NDVI_{max} - NDVI_{min}}) \qquad \text{(Kogan, 1990)} \tag{2.22}$$

When values range:

→ From 50% to 100% it indicates that vegetation is above normal.

→ From 35% to 50% it indicates a condition of drought.

→ Less than 35% then it is a severe drought condition indication (Dutta et al. 2015; Kogan 1995) (Figure 2.5) shows the values of VCI for different leaf reflectors.

VCI has two main advantages, the first that it is satellite-based so it provides us with almost real-time drought data all over the world with a reasonable resolution, the second is that it is independent from meteorological stations data since it has its own drought monitoring system (Quiring & Ganesh, 2010) .

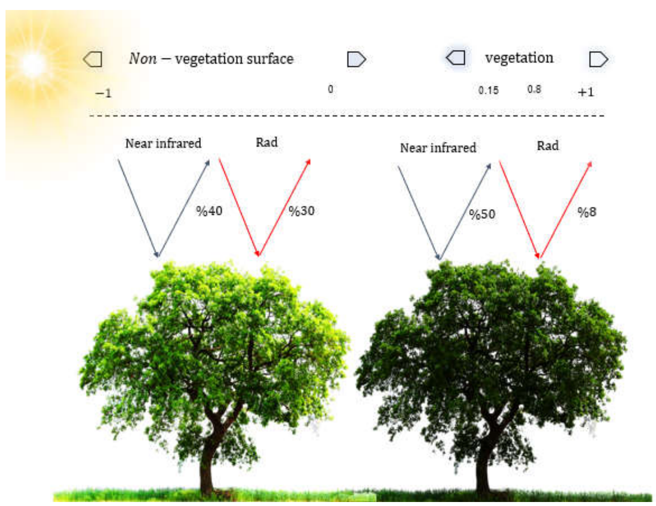

Figure 2.5. *Values of VCI for different leaf reflectors*

2.3. FAO Penman-Monteith equation

FAO established the Penman-Monteith method to estimate ETo the (R. G. Allen et al., 1998) (2.26) which was derived based on Penman-Monteith equation (2.23), aerodynamic equation (2.24), and surface resistance equation (2.25):

$$\lambda ET = \Delta \frac{(R_n - G) + P_a C_p \frac{e_s - e_a}{r_a}}{\Delta + \gamma \left(1 + \frac{r_s}{r_a}\right)} \tag{2.23}$$

Where

R_n is the net radiation.

G is the soil heat flux.

g is the psychrometric constant.

D represents the slope of the saturation vapor pressure temperature relationship.

C_p is the specific heat of the air.

(e_s - e_a) represents the vapor pressure deficit of the air.

r_a is the mean air density at constant pressure.

r_s and r_a are the (bulk) surface and aerodynamic resistances.

$$ra = \frac{ln\left(\frac{Z_m - d}{Z_{0m}}\right) ln\left(\frac{Z_h - d}{Z_{0h}}\right)}{K^2 U_Z} \quad (2.24)$$

Where

r_a is the aerodynamic resistance [s m^{-1}].

K is von Karman's constant, 0.41 [-].

u_z is the wind speed at height z [m s^{-1}].

Z_h height at which humidity measurements was taken [m].

Z_{0m} roughness length governing momentum transfer [m].

Z_{0h} roughness length governing transfer of heat and vapour [m].

Z_m is the height at which wind measurements was taken [m].

d the zero-point assumed of the plane displacement height [m].

$$rs = \frac{r_1}{LAI_{activ}} \quad (2.25)$$

Where

rs is the bulk surface resistance [s m^{-1}].

r_1 is the bulk stomatal resistance of the leaf that had enough lighting [s m-1].

LAI_{activ} is active leaf area index that is sunlit [m^2 (leaf area) m^{-2} (soil surface)].

$$ET_0 = \frac{0.408\Delta(R_n - G) + \gamma \frac{900}{T + 273} U_2(e_s - e_a)}{\Delta + \gamma(1 + 0.34u_s)} \quad (2.26)$$

Where

ET_0 reference evapotranspiration [mm day^{-1}], G soil heat flux density [MJ m^{-2} day^{-1}], T mean daily air temperature at 2 m height [°C], D slope vapor pressure curve [kPa °C^{-}

^{1}], g psychrometric constant [kPa °C^{-1}], R_n net radiation at the crop surface [MJ m^{-2} day^{-1}], u_2 wind speed at 2 m height [m s^{-1}], e_s Saturation vapor pressure [kPa], e_a actual vapor pressure [kPa], ($e_s - e_a$) saturation vapor pressure deficit [kPa].

2.4. Methodology

2.4.1. Mann- Kendall's test

(Kendall, 1938) It is a non-parametric test to find out the trends for time series data when its plot is random with no obvious trend direction. For example, if a trend is decreasing then the earlier data must be denser on the average than the following data. The magnitudes of sample data are compared in this test, and not the direct data values. In this test the there is no need for the data satisfy any specific distribution. Undetected data are simply included by giving them a value that is smaller than the minimum measured value. It makes sure that one data value only exists per time. When several data exist for a specific time, then the average value is considered.

- Test requirements:

The following suggestions should be taken into account for the Mann- Kendall's test. When there is no trend then the observations data are not serially correlated over time. These data represent the true conditions at the time of sampling. The methods of collecting and measuring samples, should represent of all phenomena over time. The measurements do not have to be normally distributed, and if there is a trend it is not necessary to be linear. The test performance can be affected with missing data, or if the values are below the limits of detection. For the data to be independent, the time between samples must be long enough, so that no correlation between measurements exists.

2.4.1.1. Calculation of the Mann-Kendall statistics (S)

The null hypothesis H0 in this test means that the trend does not exist (the data is in random order), while the alternative hypothesis H1, indicates that there is a trend. To compute the Mann Kendall test, a number of 'n' time series data points are considered, and xi and xj as two subsets of data where i = 1,2,3, …, n-1 and j = i+1, i+2, i+3, …, n. The data values are then evaluated as an ordered time series. Each data value is then checked against all the data values that follow. If a later data value is higher than an earlier one, then statistic S is increased by 1, and, if the data value from a later time period is less than an earlier one, then S is decreased by 1. The final value of S is the net sum of all adds and subtracts. The Mann-Kendall S Statistic equation is:

$$S = \sum_{i=1}^{n-1} \sum_{j=i+1}^{n} sign(Tx_j - x_i) \tag{2.27}$$

$$\mathrm{sign}(\mathrm{T_j} - \mathrm{T_i}) = \begin{cases} +1 & \text{if} \quad \mathrm{x_j} - \mathrm{x_i} > 0 \\ 0 & \text{if} \quad \mathrm{x} - \mathrm{x} = 0 \\ -1 & \text{if} \quad \mathrm{x_j} - \mathrm{x_i} < 0 \end{cases} \tag{2.28}$$

Where T_j and T_i are the annual values of the year j and i respectively, j>i. When the number of positive differences between earlier and later measurements is more than negative ones then the value of S is positive, predicting an upward trend over time. However, when the number of negative differences between earlier and later measurements is more than positive ones then the value for S negative, predicting a downward trend. When the number of positive and negative differences is almost the same, then the value of S is close to zero. This is expected when measurements are randomly existing around a constant mean with no clear trend.

If n <10, the value of |S| is compared to the theoretical distribution of S derived by Mann and Kendall. The two tailed test is used in Mann Kendall test. The trend significance needs to be statistically quantified, so the computation of the probability related to S and the sample size, n, is needed.

2.4.1.2 . Calculation of probability associated with the Mann-Kendall statistics

If the absolute value of S equals or more than the value of Sα/2 then the probability level H0 is discarded, while H1 is accepted, where Sα/2 is the smallest S which has the probability less than α/2 to appear in case of no trend. A positive or a negative value of S refers to an upward or downward trend. A normal-approximation test can be used for datasets with more than 10 values, as long as there are not many tied values within the data set. The test procedure is that for n ≥ 10, the statistic S is approximately normally distributed with the mean and variance as follows:

The variance $Var(s)$ for the S-statistic is defined by:

$$Var(s) = \frac{n(n-1)(2n+5) - \sum t_i(i)((i-1)(2i+5)}{18} \tag{2.29}$$

Normalized test statistic Z is computed as follows:

$$Z_S = \begin{cases} \frac{s-1}{\sigma} \; for\; s > 0 \\ 0 \; for\; s = 0 \\ \frac{s+1}{\sigma} \; for\; s < 0 \end{cases} \tag{2.30}$$

Z_S is used as a measure of significance of the trend. This test statistic is used to test the null hypothesis, H0. If | Zs| is larger than Zα/2, where α is the chosen significance level (e.g.: 5% with Z 0.025 = 1.96) so the null hypothesis is invalid which prove the trend to be significant.

2.4.2. Theil-Sen's slope estimator

The Theil-Sen's nonparametric method is used to find out the slope of a trend (P. K. sen, 1968; Theil, 1950). In those cases where the trend can be considered to be linear the Sen's method can be used, $f(t)$ is:

$$f(t) = Qt + B \tag{2.31}$$

Where Q is the slope and B is a constant. To get the slope estimate Q in equation (2.31), the slopes of all data value pairs are calculated.

$$Q_i = \frac{x_j - x_k}{j - k} \tag{2.32}$$

Where j>k. If there are n values x_j in the time series, we get as many as N = n(n-1) /2 slope estimates Q_i. The average of these N values of $Q_i$is the Sen's estimator of slope. Then we rank the N values of Q_i from the smallest to the largest and the Sen's estimator is:

$$Q = Q_{\left[\frac{N+1}{2}\right]} \quad ,if\ N\ is\ odd\ or\ \ Q = \frac{1}{2}\left(Q_{\left[\frac{N}{2}\right]} + Q_{\left[\frac{N+2}{2}\right]}\right), if\ N\ is\ even \tag{2.33}$$

2.4.3. Pettitt's test

The non-parametric approach after (Pettitt, 1979) is used to find out a the change-point in the series of continuous hydrological, or climate data. It tests the H0-hypothesis (no change) against the Ha-Hypothesis, (change) to detect a specific time (t) from which the variables either decrease or increase. A reasonable non-parametric test to detect a change uses a version of the Mann-Whitney two-sample

$$\mathrm{D_{ij}} = \mathrm{sign}(\mathrm{x_j} - \mathrm{x_i}) \tag{2.3420}$$

$$\mathrm{sign}(x_j - x_i) = \begin{cases} +1 & \text{if} \quad x_j - x_i > 0 \\ 0 & \text{if} \quad x - x = 0 \\ -1 & \text{if} \quad x_j - x_i < 0 \end{cases} \tag{2.35}$$

$$U_{t.T} = \sum_{i=1}^{t} \sum_{j=t+1}^{T} D_{ij} \tag{2.36}$$

Where $U_{t.T}$ is equivalent to a Mann-Whitney statistic for tow samples x_1 ..., x_t and x_{t+1}, ..., x_T come from the same population.

Then $U_{t.T}$ is checked for values of t with $1 \leq t < T$. The most probable change point is the one with a maximum value of $U_{t.T}$:

$$K_T = \max_{1 \leq t \leq T} |U_{t.T}| \tag{2.37}$$

The probability of the change point is calculated using

$$p \cong \exp\left(\frac{-6K_T^2}{T^3 + T^2}\right) \tag{2.38}$$

CHAPTER 3
RESULTS AND DISCUSSION

3.1. Performance of Trend Analysis

To perform the trend analysis, the Mann–Kendell's test, Sen's slope test, and Pettitt's test were applied to SPEI values for 1-3-6, and 12 time-scales for 1901-2015 time-periods. As recommended in the study of (Hadi & Tombul, 2018) that the period from 1901-2015 was to be divided into two or more periods, we divide it into two periods in this study (1901-1981), and (1982-2015). The change point in Turkey was considered to be the period that follows 1985 because of the great increase of economic and industrial development, which is a reason for significant climate change (Unal, Deniz, Toros, & Incecik, 2012). The trend was studied before and after 1982, because the VCI data covers only from January-1982 since the monthly data of the year of 1981 are not complete so it was removed. Then the trend analysis was applied to VCI data for the 1982-2015 period.

3.2. Trend Analysis of SPEI for the Period from 1901-2015

3.2.1. SPEI-1 time -scale

Mann –Kendell's analysis for SPEI-1 data for the 1901–2015 period shows that; for the 1-month time-scale (short range time-scale), the whole SEA area, the southwestern parts of Turkey, as well as the central parts of EA have significant negative MK-z values indicating an important negative change of SPEI-1values, noting a change towards drought, where the maximum negative MK-z values are in southern SEA. While in western and some central parts of BS, western parts of MA, and northern AE, significant positive MK-z values can be noticed, noting a wetter weather with time, where the maximum positive MK-z values are in northern BS. Other areas show insignificant MK-z values. The confidence level of all MK-z values is at 0.05 (Figure 3.1.a).

Sen's slope test shows that slope values gradually increased (negatively and positively towards the southeastern and northwestern parts of the country where the maximum negative value is -0.00043 in southern SEA, and the maximum positive value is 0.00025 in northern BS (Figure 3.2.a).

The most probable year of change was not detected as a dominant single year in the grids, but the most noted year of change is 1953 that was noticed in 27 grids, 1925 follows with being noticed in 18 grids (Figure 3.3.a).

3.2.2. SPEI-3 time-scale

Mann –Kendell's analysis for SPEI-3 data for the 1901–2015 period shows that for the 3-month time-scale (seasonal time-scale), the whole SEA areas, parts of southern MD, the southeastern and northeastern parts, and some parts of central EA, have significant negative MK-z values indicating a general trend towards drought in the direction of the southeast of Turkey, where the maximum negative MK-z values are in the southeastern EA, and southern SAE. While in MA area, western and some central parts of BS, northwestern and northeastern parts of CA, and northern AE, significant positive MK-z values can be noticed, noting a wetter weather with time, where the maximum positive MK-z values are in northwestern parts BS, and eastern MA. The confidence level of all MK-z values is at 0.05 (Figure 3.1.b).

As in SPEI-1, the Sen’s slope test shows that slope values gradually increased (negatively and positively) towards the southeastern and northwestern parts of the country where the maximum negative value is -0.00035 in southern SEA, and the maximum positive value is 0.00035 in northwestern BS, and northeastern MA (Figure 3.2.b).

The most probable year of change was not detected as a dominant single year in the grids, but same as SPEI-1 the most noted year of change is 1953 which was noticed in 27 grids. The year 1993 follows with being noticed in 23 grids (Figure 3.3.b).

3.2.3. SPEI-6 time-scale

Mann –Kendell's analysis for SPEI-6 data for the 1901–2015 period shows that for the 6-month time-scale (medium range time-scale), the whole SEA area, central and parts of southern MA, the South eastern, central and western EA, have significant negative MK-z values indicating a general trend towards drought, where the maximum negative MK-z values are in southern EA, SAE, and MD areas. While in MA area, and most parts of BS, northeastern and western AE, western and eastern parts of CA, and western EA significant positive MK-z values can be noticed, noting a wetter weather with time. The confidence level of all MK-z values is at 0.05 (Figure 3.1.c).

The Sen’s slope test shows that slope values gradually increased (negatively and positively) towards the southeastern and northwestern parts of the country where the maximum negative value is -0.0055, and the maximum positive value is 0.0005 in northern CA (Figure 3.2.c).

The most probable year of change was not detected as a dominant single year in the grids, but the most noted year of change is 1968 that was noticed in 26 grids. Same as in SPEI-3 the year 1953, follows with being noticed in 23 grids, then the year 1993 is noticed in 20 grids (Figure 3.3.c).

3.2.4. SPEI-12 time-scale

Mann –Kendell's analysis for SPEI-12 data for the 1901–2015 period shows that for the 12-month time-scale (long range time-scale), the whole SEA area, southeastern EA, southern CA, south western AE, and most parts of MA, have significant negative MK-z values indicating a general trend towards drought, where the maximum negative MK-z values are in southern EA, SEA, and MD areas. While in MA, BS, northern AE, eastern and northwestern parts of CA, and northwestern EA significant positive MK-z values can be noticed, noting a wetter weather with time, where the maximum positive values were in northeastern CA, northeastern MA, and northwestern BS (Figure 3.1.d). The Sen’s slope test shows that slope values ranged from -0.0007 in southern MD to 0.00065 in northern MA. The confidence level of all MK-z values is at 0.05 (Figure 3.2.d).

According to (Figure 3.3.d) the most probable year of change was not detected as a dominant single year in the grids, but same as SPEI-6 the most noted year of change is 1968 which was noticed in 42 grids, and same as in SPEI-1 the year 1925 follows with being noticed in 27 grids, then the year 1961 is noticed in 18 grids.

The line that separates positive and negative trend areas in the western part of Turkey is displaced to the north as we shift from SPEI-1 to SPEI-12 Time scale. While in the far west of the Marmara and Aegean regions it shifts to the west with the increment of SPEI series time-scale from 1 to 12. However, in the eastern part it was noticed that it shifted south as we go from the SPEI-1 to SPEI-3 to SPEI-6 time-scales and shifted north at SPEI-12 time-scale (Figure 3.4).

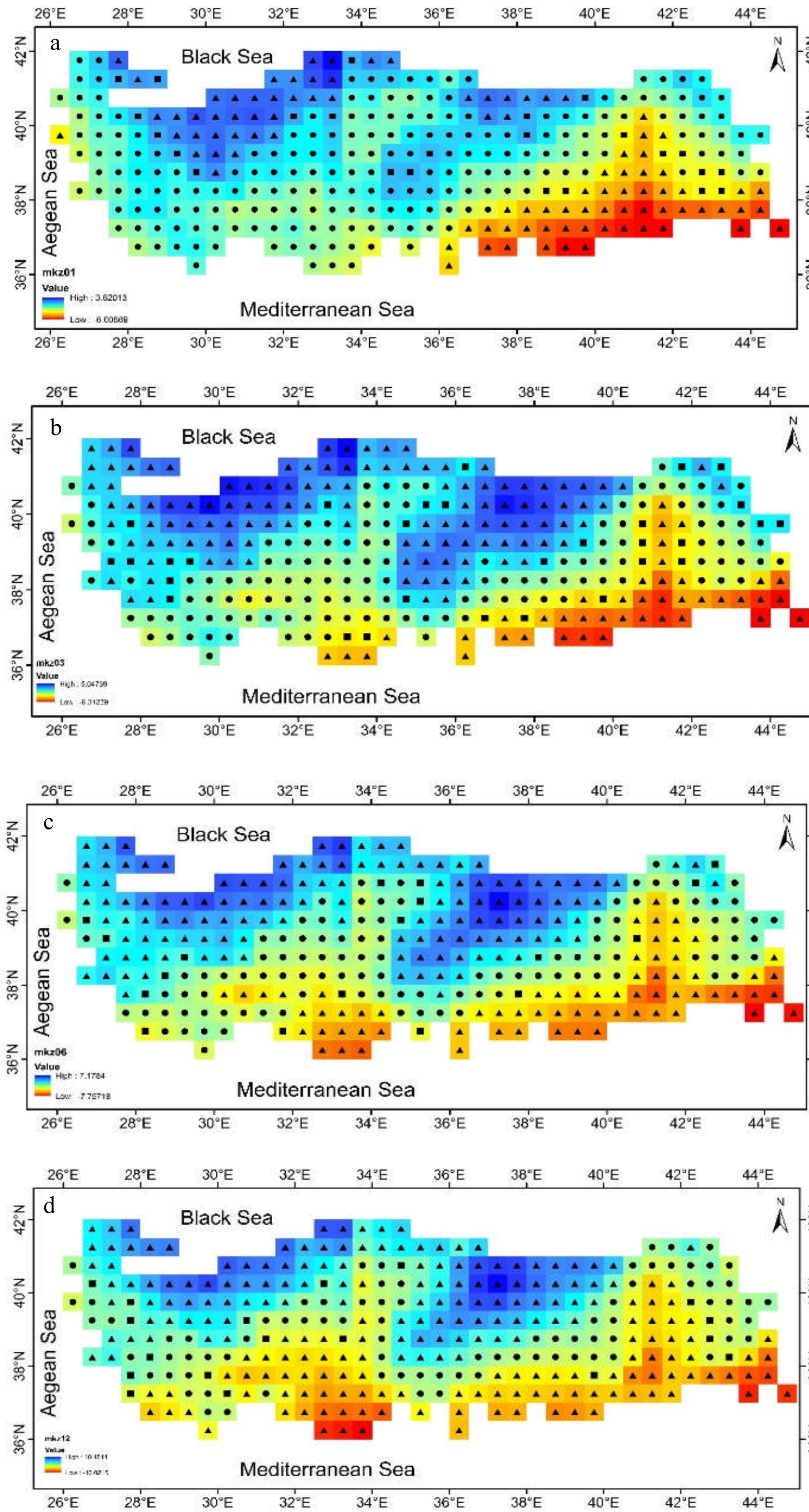

Figure 3.1. *Spatial variation of MK-Z value of the SPEI trend test data for the 1901–2015 period (a: 1-month, b: 3-month, c: 6-month, d: 12-month). Grid size is 0.5 degree × 0.5 degree. Grids with dots represent statistically insignificant trends, squares represent significant trends with confidence level of 90%, triangles represent significant trends with confidence level of 95%.*

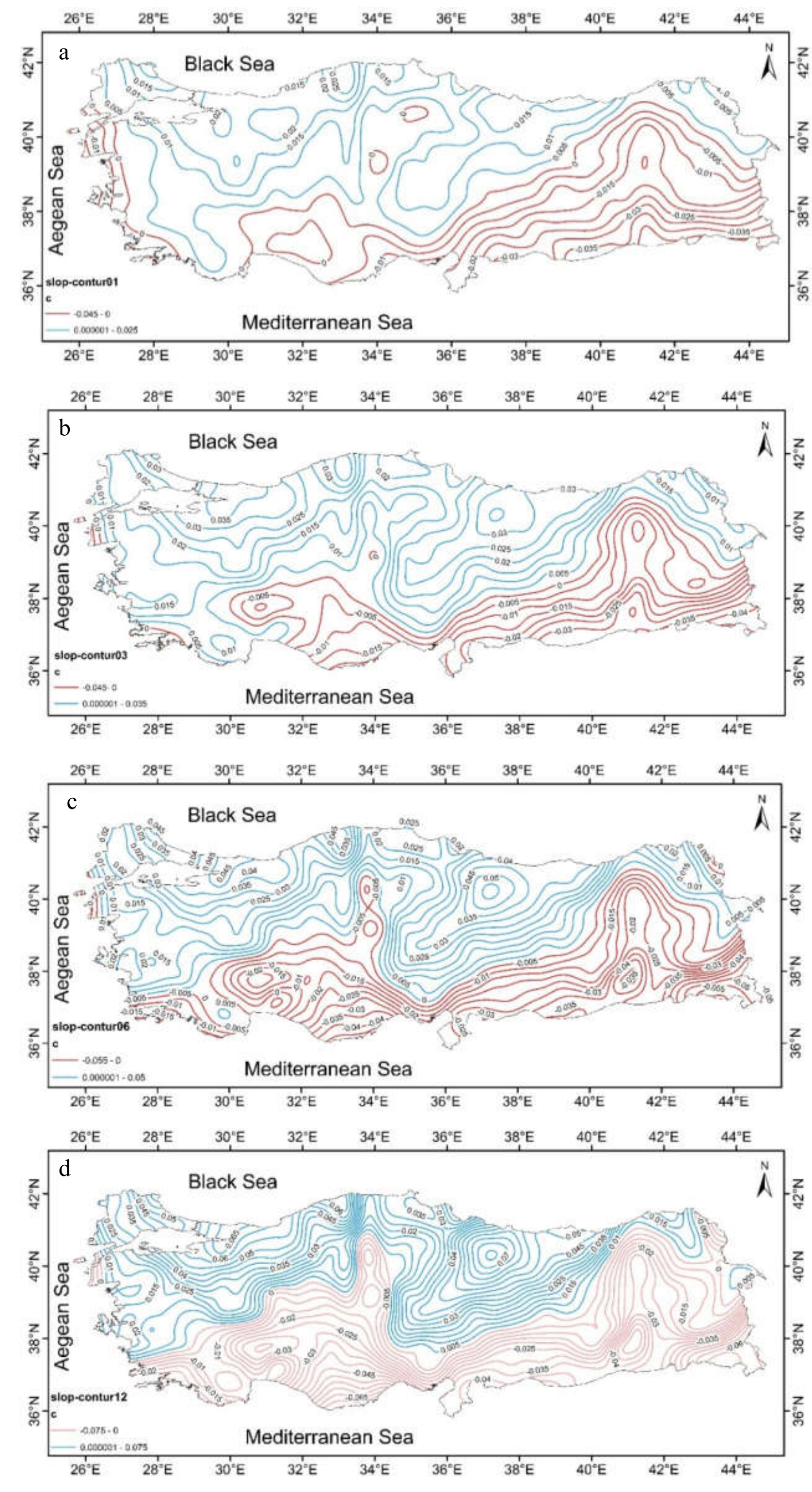

Figure 3.2. *Contour lines for the spatial distribution of the Theil-Sen test slope values (*10^-2) of the SPEI trend test data for the 1901–2015 period (a: 1-month, b: 3-month, c: 6-month, d: 12-month).*

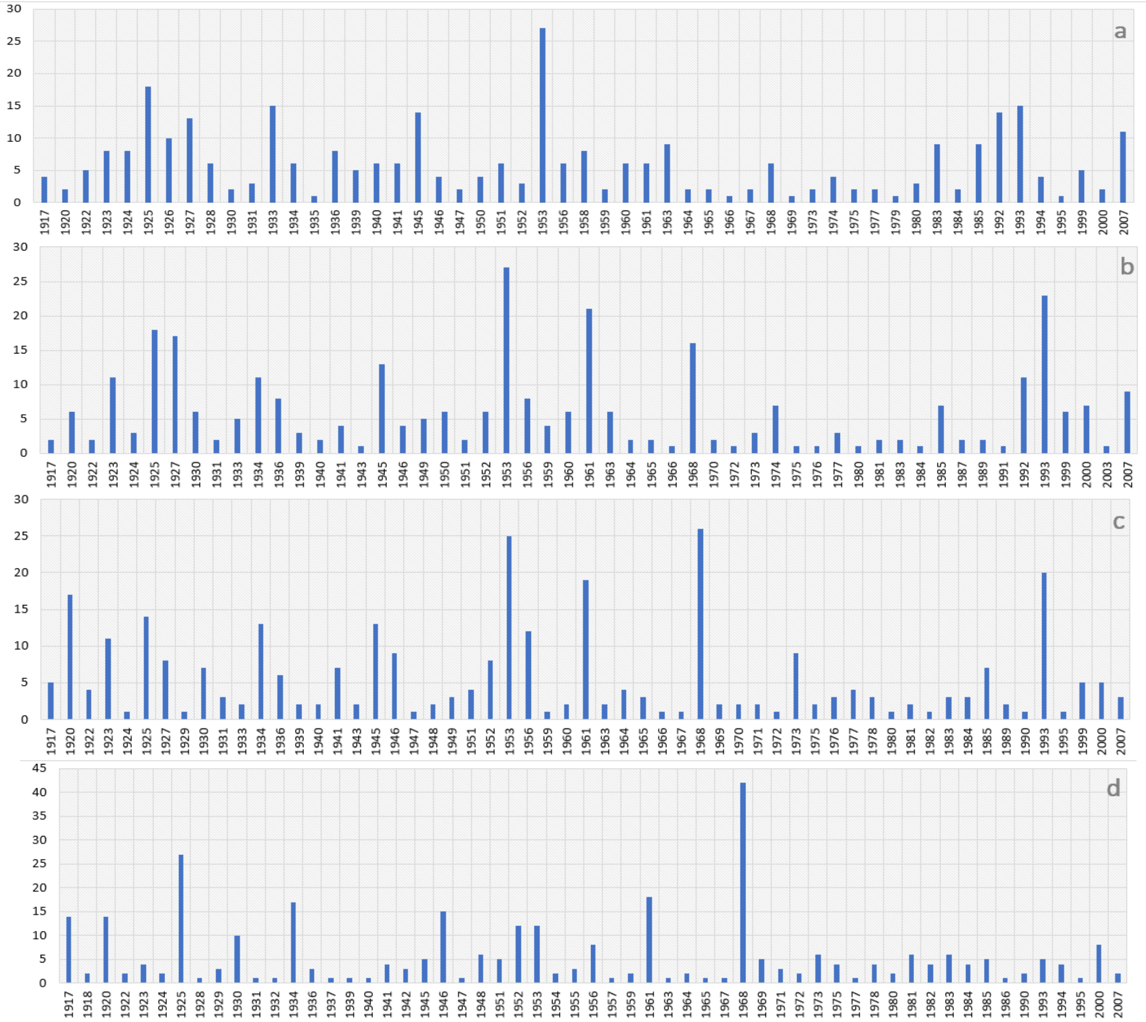

Figure 3.3. *Results of the Pettitt's test on SPEI trend test data for the 1901–2015 period*

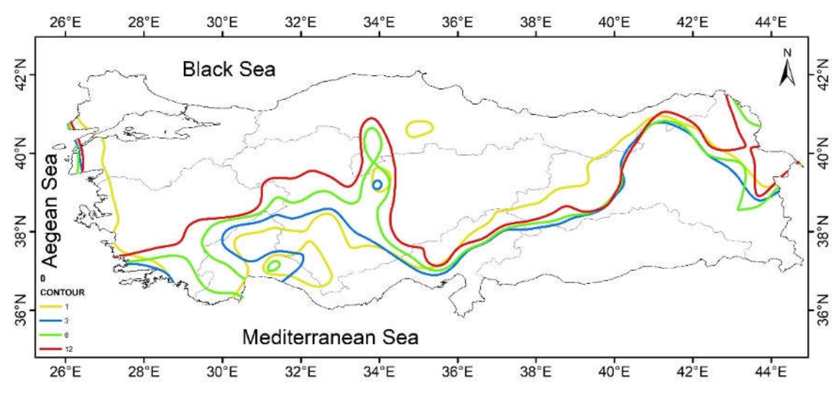

Figure 3.4. *The zero-value Contour lines of the Theil-Sen test for the 1901–2015 period showing how they shift according to the time-scale*

3.3. Trend Analysis of SPEI for the Period from 1901-1981

3.3.1. SPEI-1 time-scale

The significant positive MK-z values were noticed at the west of the BS region and east of MA, while significant negative MK-z values can be noticed at the SEA and southeastern of EA region. Other areas show insignificant MK-z values (Figure 3.5.a). Sen's slope maximum negative value is -0.0006 in the south of SEA region, and the maximum positive value is 0.00035 in northern BS region. The confidence level of all MK-z values is at 0.05 (Figure 3.6.a).

The most probable year of change was not detected as a dominant single year in the grids, but the most noted year of change is 1927 which was noticed in 28 grids, the years (1924,1925) follow with being noticed in 24 grids (Figure 3.7.a).

3.3.2. SPEI-3 time-scale

The significant positive MK-z values were noticed at the west and middle of the BS region, MA region, and north of AE region, while significant negative MK-z values can be noticed at the east of EA region and south of both of SEA region and ME region. Other areas show insignificant MK-z values (Figure 3.5.b). As in SPEI-1, Sen's slope maximum negative value is -0.0004 in the east of EA and -0.00035 in the south of SEA region, and the maximum positive value is 0.00055 in northern BS region. The confidence level of all MK-z values is at 0.05 (Figure 3.6.b).

The most noted year of change is 1953, which was noticed in 29 grids, the years (1925,1927) follow with being noticed in 28 grids (Figure 3.7.b).

3.3.3. SPEI-6 time-scale

The significant positive MK-z values were noticed at the MA region, north of AE region, and the far east of western BS region. While significant negative MK-z values can be noticed at the middle of BS region, north CA region, east of MD region, and east of EA region. (Figure 3.5.c). As in SPEI-3, Sen's slope maximum negative value is -0.00055 in the east of EA region and south of MD region, while the maximum positive value is 0.0007 in northern BS region. The confidence level of all MK-z values is at 0.05 (Figure 3.6.c).

The most noted year of change is 1925, which was noticed in 51 grids, the year 1953 follows with being noticed in 24 grids (Figure 3.7.c).

3.3.4. SPEI-12 time-scale

The significant positive MK-z values were noticed at west part of Turkey. While significant negative MK-z values can be noticed in central Turkey (middle of BS region, CA region, MD region), and in the far east of EA region (Figure 3.5.d). Sen's slope test show that slope maximum negative value is -0.0009 in the east of EA region while the maximum positive value is 0.00095 in the east of MA region (Figure 3.6.d). The most noted year of change is 1925, which was noticed in 48 grids, the year 1934 follows with being noticed in 32 grids. The confidence level of all MK-z values is at 0.05 (Figure 3.7.d).

(Figure 3.8) shows the Displacement of the line separating positive and negative trend areas.

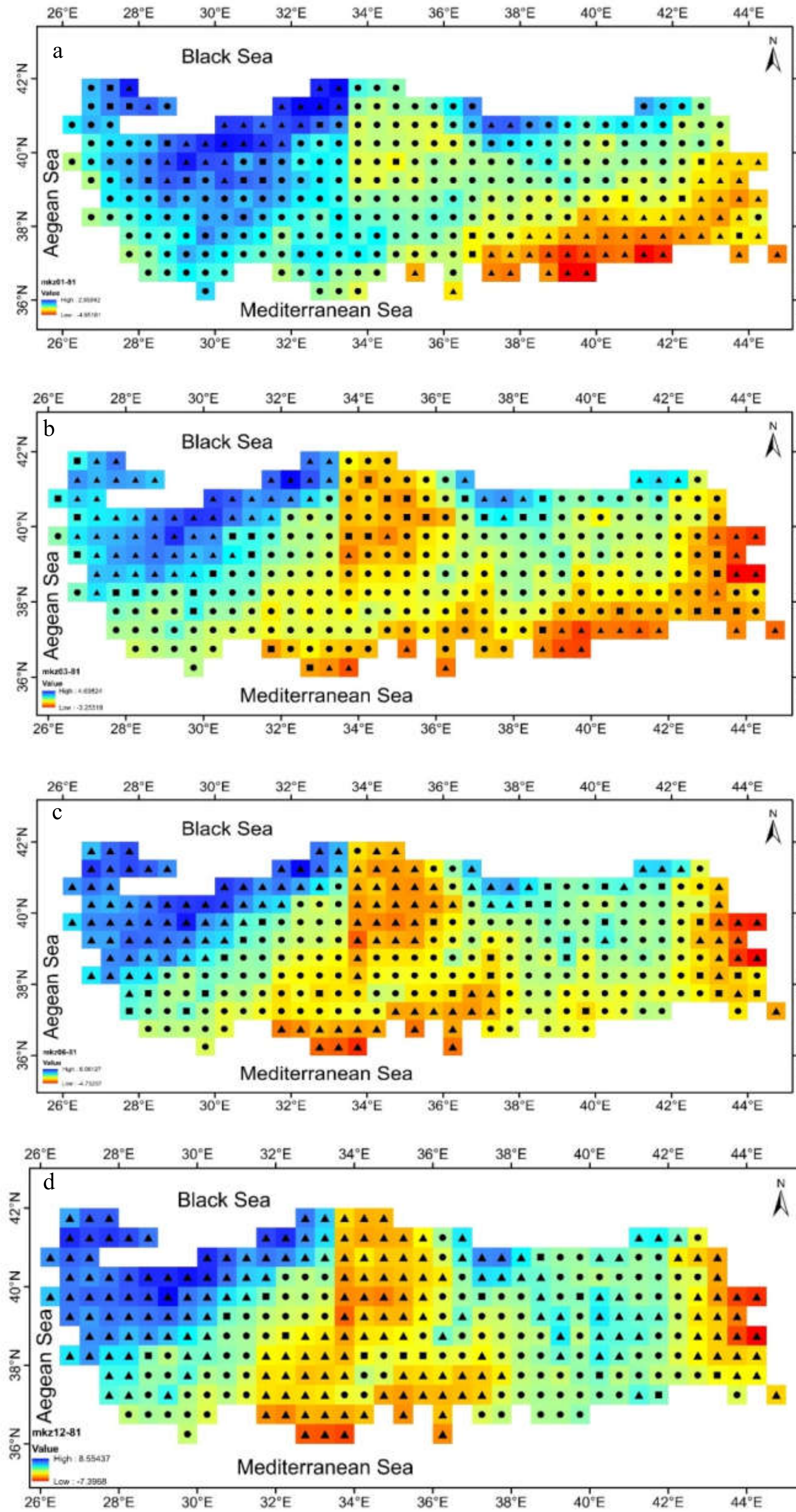

Figure 3.5. *Spatial variation of MK-Z value of the SPEI trend test data for the 1901–1981 period (a: 1-month, b: 3-month, c: 6-month, d: 12-month). Grid size is 0.5 degree × 0.5 degree. Grids with dots represent statistically insignificant trends, squares represent significant trends with confidence level of 90%, triangles represent significant trends with confidence level of 95%.*

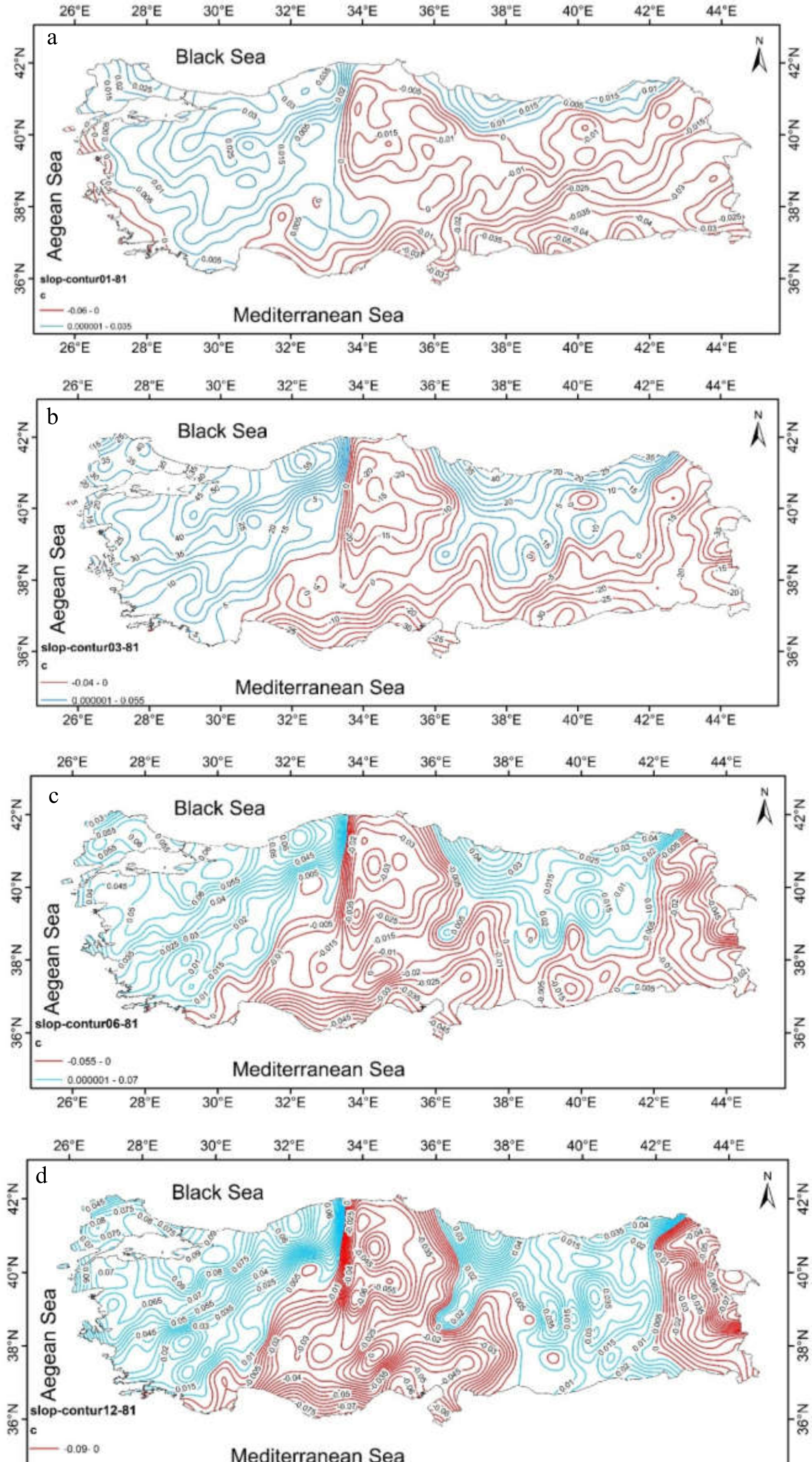

Figure 3.6. *Contour lines for the spatial distribution of the Theil-Sen test slope values (*10^-2) of the SPEI trend test data for the 1901–1981 period (a: 1-month, b: 3-month, c: 6-month, d: 12-month).*

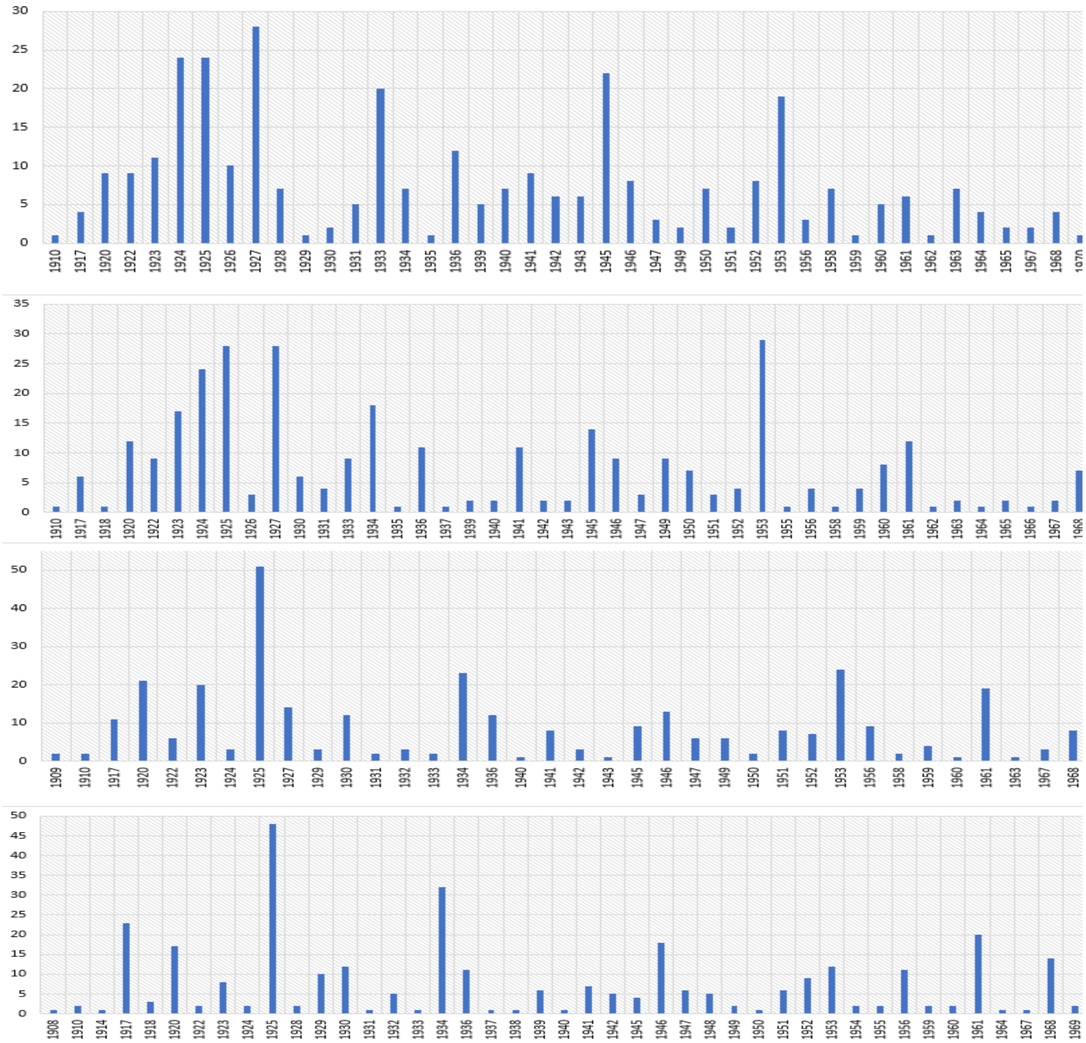

Figure 3.7. *Results of the Pettitt's test on SPEI trend test data for the 1901–1981 period*

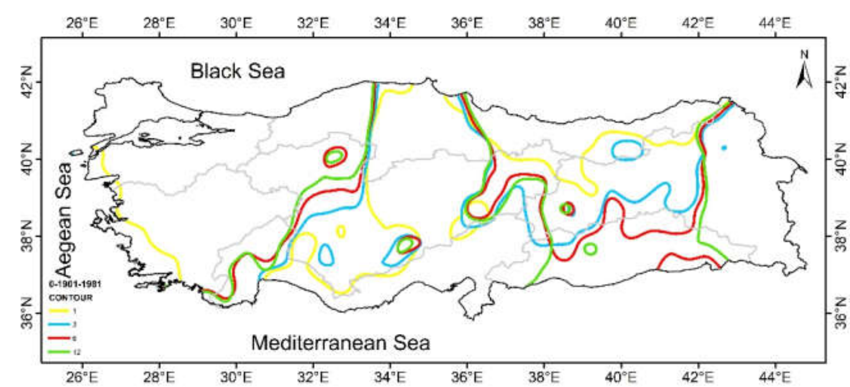

Figure 3.8. *The zero-value Contour lines of the Theil-Sen test for the 1901–1981 period showing how they shift according to the time-scale.*

3.4. Trend Analysis of SPEI for the Period from 1981-2015

3.4.1. SPEI-1 time-scale

The significant positive MK-z values were noticed in the western part of the Marmara region, southeastern of Central Anatolia region, and northern of the Mediterranean region. While the remaining regions are insignificant (Figure 3.9.a). The Sen's slope test show that most areas have a positive slope, and the maximum positive value is +0.0021 in the west of the Aegean region, while negative slope extended from the southern Anatolia region to the center of the Southeastern Anatolia region and from the center of the Eastern Anatolia region to the north, and the maximum negative value is -0.0012 in the Southeastern Anatolia region. The confidence level of all MK-z values is at 0.05 (Figure 3.10.a).

The most probable change year is 2007, which was noticed in 83 grids, the year 1993 follows with being noticed in 57grids (Figure 3.11.a).

3.4.2. SPEI-3 time-scale

The significant positive MK-z values were noticed in Marmara region, Aegean region, most areas of Central Anatolia region and the Mediterranean region, northern part of Eastern Anatolia region, while the remaining regions are insignificant (Figure 3.9.b). Sen's slope test shows that slope maximum negative value is -0.0016 in the northeast of Eastern Anatolia region while the maximum positive value is 0.0038 in the west of Marmara region. The confidence level of all MK-z values is at 0.05 (Figure 3.10.b).

Same as SPEI-1 the most noted year of change is 2007, which was noticed in 103 grids. The year 1993 follows with being noticed in 71 grids (Figure 3.11.b).

3.4.3. SPEI-6 time-scale

The significant positive MK-z values were as same as SPEI-3 with increasing prevalence over more areas (Figure 3.9.c). The Sen's slope test shows that slope maximum negative value is -0.0025 in the middle of Southeastern Anatolia region while the maximum positive value is 0.005 in the west of Marmara region. The confidence level of all MK-z values is at 0.05 (Figure 3.10.c).

Same as SPEI-1 and SPEI-3 the most noted year of change is 2007, which was noticed in 103 grids. The year 1993 follows with being noticed in 89 grids (Figure 3.11.c).

3.4.4. SPEI-12 time-scale

The significant positive MK-z values are in most regions, while the significant negative MK-z values are in parts of the middle of Southeastern Anatolia and Eastern Anatolia (Figure 3.9.d). The Sen's slope test shows that maximum negative value is -0.0036 in the middle of Southeastern Anatolia region, while the maximum positive value is 0.0057 in the west of Marmara region. The confidence level of all MK-z values is at 0.05 (Figure 3.10.d).

The most probable change year is 1993, which was noticed in 97 grids, the year 2007 follows with being noticed in 94 grids (Figure 3.11.d).

(Figure 3.12) shows the Displacement of the line between positive and negative trend areas.

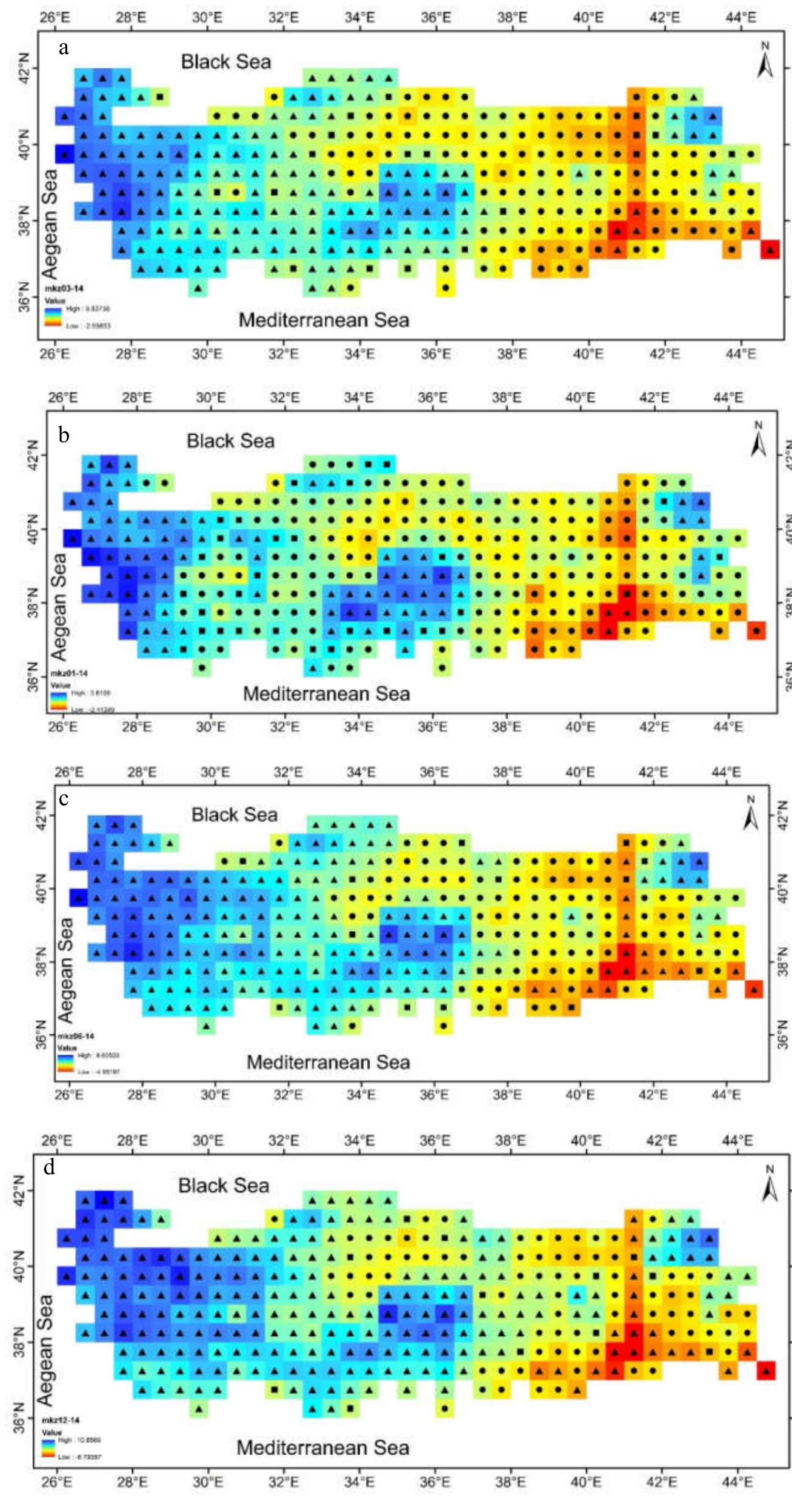

Figure 3.9. *Spatial variation of MK-Z value of the SPEI trend test data for the 1982–2015 period (a: 1-month, b: 3-month, c: 6-month, d: 12-month). Grid size is 0.5 degree × 0.5 degree. Grids with dots represent statistically insignificant trends, squares represent significant trends with confidence level of 90%, triangles represent significant trends with confidence level of 95%*

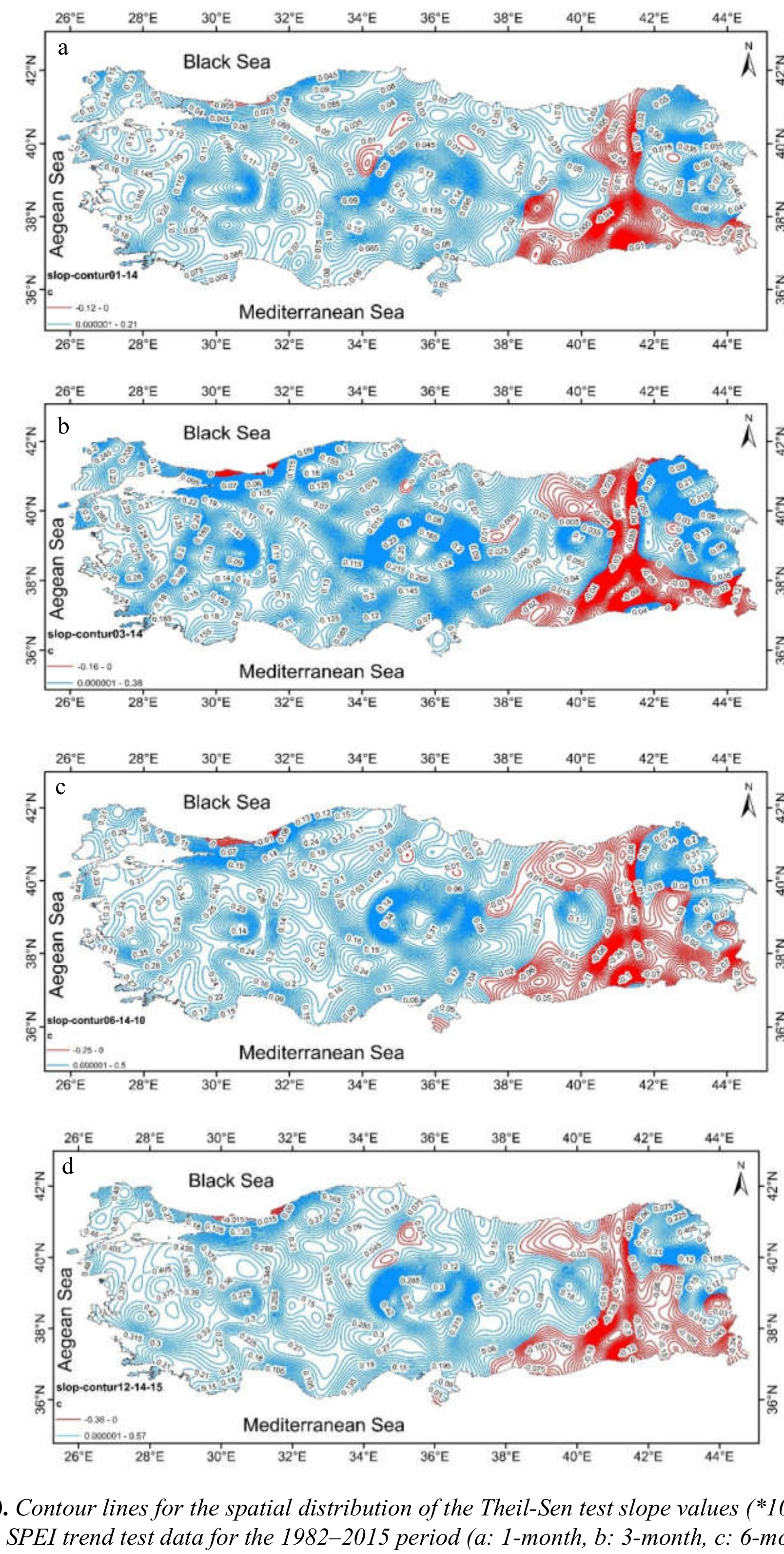

Figure 3.10. *Contour lines for the spatial distribution of the Theil-Sen test slope values (*10^-2) of the SPEI trend test data for the 1982–2015 period (a: 1-month, b: 3-month, c: 6-month, d: 12-month).*

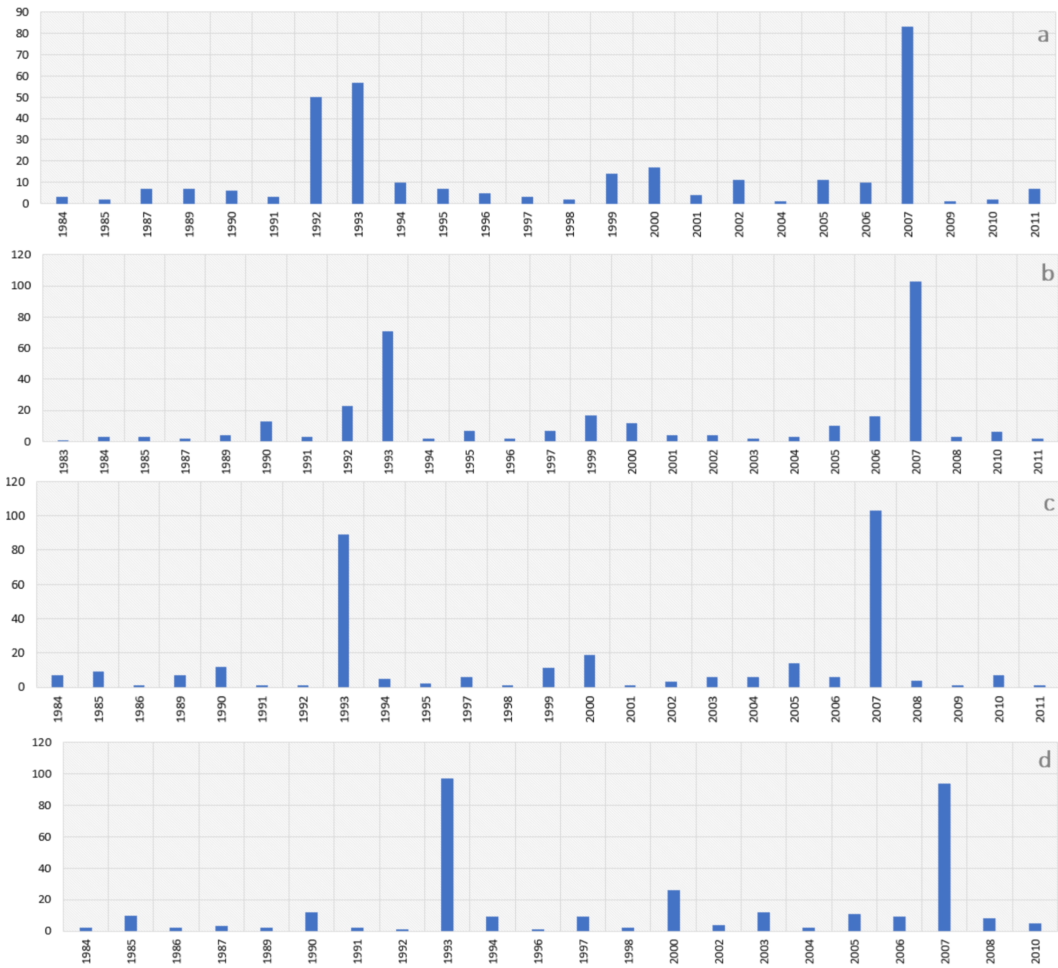

Figure 3.11. *Results of the Pettitt's test on SPEI trend test data for the 1982–2015 period).*

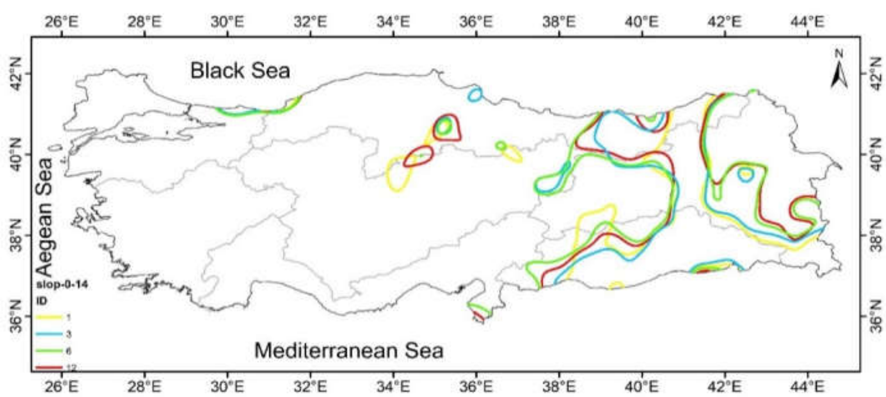

Figure 3.12. *The zero-value Contour lines of the Theil-Sen test for the 1982–2015 period showing how they shift according to the time-scal*

3.5. Trend Analysis of VCI for the Period from 1981-2015

Mann–Kendell's analysis for VCI data for the 1901–2015 period shows that almost all regions of Turkey have negative MK-z values indicating an important positive change of VCI values, which implies a decrease in agricultural drought, however; negligible negative MK-z values were observed in the far northeast of Turkey. The confidence level of all MK-z values is at 0.05 (Figure 3.13).

The Sen's slope test values show that almost whole regions of Turkey have positive values except for a very few parts of the far East of Eastern Anatolia region, the maximum positive value is +0.18 in the Aegean region, and the maximum negative value is -0.02 in Eastern Anatolia region (Figure 3.14).

The year 1993 was noticed in 59 grids which makes it the most recurrent year of change, the year 1996 follows with being noticed in 52 grids (Figure 3.15).

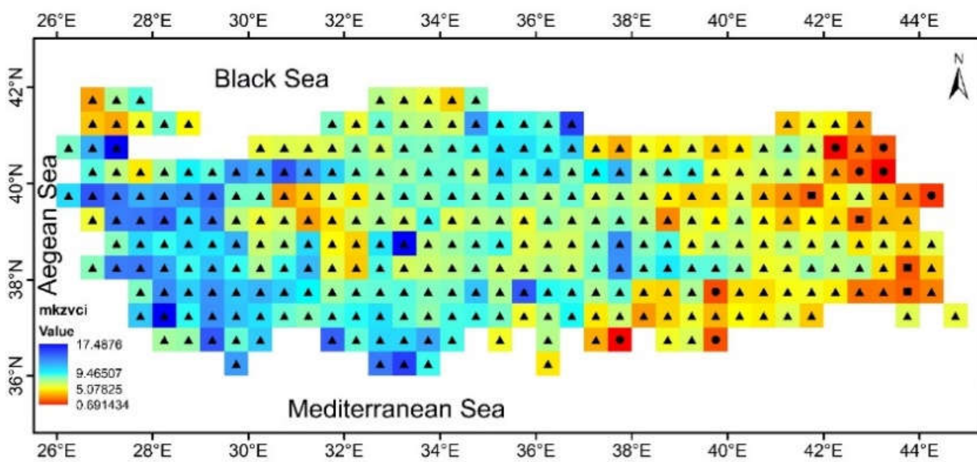

Figure 3.13. *Spatial variation of MK-Z value of the VCI trend test data for the 1982–2015 period. Grid size is 0.5 degree × 0.5 degree. Grids with dots represent statistically insignificant trends, squares represent significant trends with confidence level of 90%, tringles represent significant trends with confidence level of 95%*

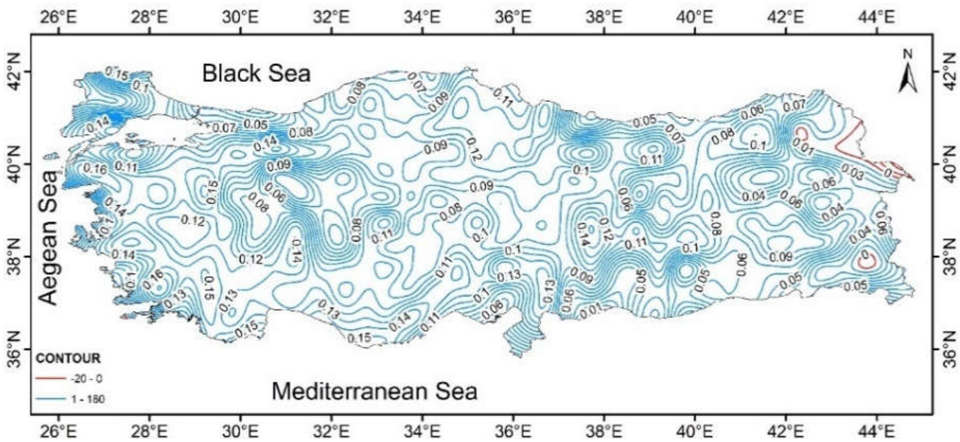

Figure 3.14. *Contour lines for the spatial distribution of the Theil-Sen test slope values of the VCI trend test data for the 1982–2015 period*

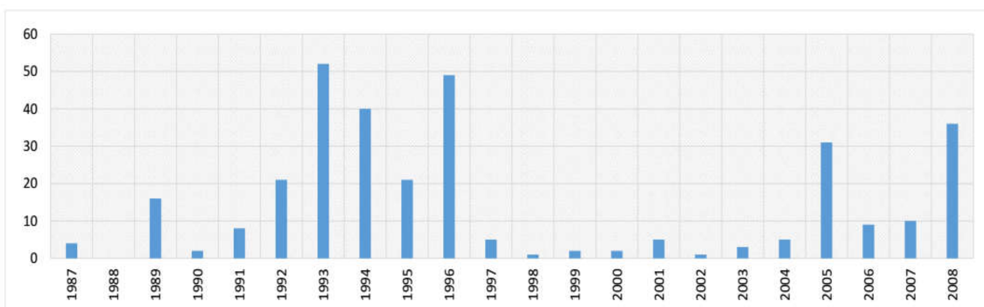

Figure 3.15. *results of the Pettitt's test on VCI trend test data for the 1982–2015 period*

3.6. Comparison Between SPEI-1 and VCI Trend Results

Both the SPEI-1 and VCI data for the period of 1982-2015 were subjected to the Mann-Kendall's test. The SPEI-1 results showed that some parts of the country were insignificant, while other parts were significant. While For VCI, most of the country was significant which is not the case for SPEI-1. Considering Sen's slope test for SPEI-1 trend, it was found that some parts of the country had a negative slope, while other parts had a positive slope, however in the case of VCI Sen's slope test, all the studied area showed a positive slope. The cause of such variation can be explained by the difference between the bases of VCI and SPEI-1 data sources. VCI is a reflective-based index (satellite-derived) that is obtained by remote sensing, while SPEI is a Meteorological-based index that is obtained from meteorological data (temperature, and precipitation). Such a disagreement between SPEI-1 and VCI indices was discussed by (Gitelson, Kogan, Zakarin, Spivak, & Lebed, 1998; Kogan, 1997; Quiring & Ganesh, 2010;

Unganai & Kogan, 1998) who stated that VCI is good for agricultural drought monitoring but poor when applied for meteorological drought, also (Bayarjargal et al., 2006; Bhuiyan et al., 2006; Singh et al., 2003; Sergio M Vicente-Serrano, 2007) agreed with that, and (Singh et al., 2003) stated that monitoring drought using VCI only is not enough, That is why (Brown, Wardlow, Tadesse, Hayes, & Reed, 2008) invented a new hybrid index that employs both station-based and satellite-based drought indices by merging them jointly and called it VegDRI index in an effort to make use of both indices with each other for a better and more reasonable results that avoid the differences between the different-based indices. Therefore, it can be concluded that VCI and SPEI are not strongly correlated and variations between them are highly expected.

3.7. Comparison of SPEI Results for Different Time Periods

Comparing the drought trend results for the periods of (1901-1981) and (1982-2015) reveals, that climate trend tends to be wetter after the year 1982. The wet trend becomes more obvious as we move from SPEI-01 to SPEI-12. Costal western parts of MA and AE showed a dryer trend prior to 1982 however changed into a wetter trend after 1982. The central and eastern parts of MD also had a change from dryer to wetter trend after 1982. BS and CA trends became wetter after 1982. The western parts of EA had a wet trend while the eastern parts had a dry trend prior to 1982, but after 1982, the central and far southeastern kept the dry trend while the eastern and western parts followed a wetter trend. SEA mainly kept the dry trend after the year 1982.

Comparing the drought trend results for the full study periods of (1901-2015) with the (1901-1981) period, which is the first part of it we can notice that the dry trend for the (1901-1981) period is higher than the overall period of (1901-2015) with the dry trend getting more obvious as we move from SPEI-1 to SPEI-12. The fact that the whole period of study (1901-2015) trend has lower tendency towards drought than the first part of it (1901-1981) makes it clear that the period after 1981 changed into a wetter trend making the full period trend of (1901-2015) less dryer. However, the southeastern SEA kept a persistent dry trend in both periods indicating a non-change trend after 1981.

Comparing the drought trend results for the full study periods of (1901-2015) with the (1982-2015) period, which is the later part of it we can notice in general that a higher tendency towards wetter trends which gets more obvious as we move from SPEI-1 to SPEI-12. However, the dry trend for the southeastern parts of Turkey keeps persistent.

The wetter trends after 1981did contribute to the overall trend for the whole period of study (1901-2015) towards less severe dry trends, or even towards wet trends in some parts of Turkey (Figure 3.16). So, there is general tendency towards a less dry or even wetter trends after the year 1981, this has to be monitored in the future to determine the future climate trends more accurately. However, in the situation in the southeastern parts of Turkey is worrying as the drought trend is more significant, sever, and persistent showing no regression even after 1981, which highlighting the serious need to consider the necessary measures to counter the expected effects of drought in the future in this area.

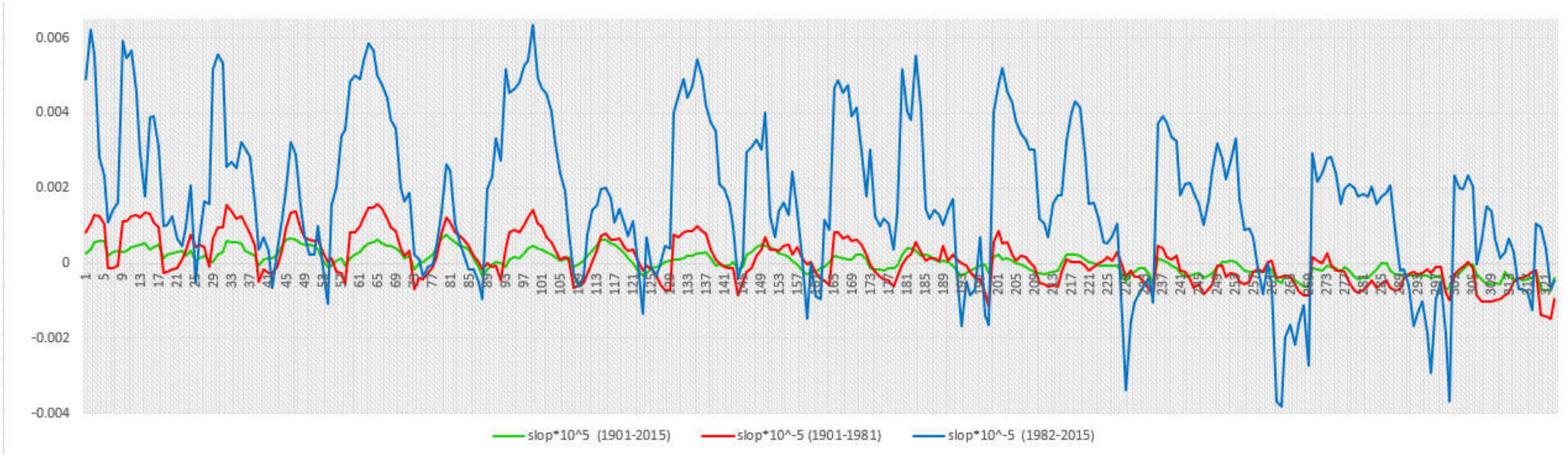

Figure 3.16 *The SPEI-12 trend slope comparison for the periods of (1901-2015), (1901-1981), and (1982-2015) for all the grid points.*

CHAPTER 4
SUMMARY, CONCLUSION AND RECOMMENDATIONS

4.1. Summary and Conclusion

In the thesis, trend analysis of SPEI was conducted for all Turkey from 1901 to 2015 and for the periods of 1901-1981, and 1982-2015 (these two periods before and after 1982 were suggested in several previous studies). Analysis trend of VCI was performed as well, covering the same area for the years 1982-2015.

The monthly values for SPEI (1,3,6,12 months) time-scales for the period of study, were taken from http://spei.csic.es/ (The Spanish National Research Council), and it was SPEI version 2.5 with a 0.5º lat/lon Spatial resolution. The FAO-56 Penman-Monteith equation was used to calculate the potential evapotranspiration. Based on the NDVI 3rd generation values from the (AVHRR) sensors of the (NOAA) satellite, the VCI values were calculated using GIMMS (Global Inventory Modeling and Mapping Studies) project.

The Mann−Kendall test was used to analyze the data to determine the direction of the trend and its significance according to their MK-z value. The Theil−Sen test estimated the trend's slope magnitude. Then the "most probable change year" was found out using the Pettitt test. The trend was analyzed using the R statistical program, and the spatial patterns of the results were done by The GIS (Geographic Information System) software.

As a result of SPEI analysis for the years from 1901-2015 a negative trend (increasing drought) was observed in the southern, southern eastern, and some central parts of Turkey, while a positive trend (a wetter trend) was in the northern, western, and some central parts of Turkey, with some exceptions within those areas. The line between the negative and positive-trend zones (zero trend zone) shifts north as the SPEI time-scale goes from SPEI-1 to SPEI-12, so longer-term drought obviously affects wider areas as the time scale goes longer. Long-term drought affects more areas of Turkey than short-term drought which affects southern, southern eastern, and some central parts, however some areas with wet trend at the shorter time-scale are suffering long-term drought. These analysis results are Compatible with (Hadi & Tombul, 2018) for Annual trend Precipitation where southeastern Anatolia and the Mediterranean have a negative trend while the Black Sea and Marmara regions have a positive trend. The most probable year of change is 1968 For SPEI-6, which is the same as in SPEI-3, and the year 1953, follows, then the year 1993, which resembles the findings of (Hadi & Tombul, 2018) as the most probable year of change for the annual temperature trend. For both SPEI-12, and SPEI-6 the most probable year of change is 1968, which was also concluded by (Hadi & Tombul, 2018).

The trend analysis results show that there is a distinct difference before and after 1982. Before 1982 a spatial wide spread for negative trend (more drought) for the whole eastern and central Turkey extending from north to south for SPEI-1 while it retreats south with increasing time-scale to conclude only the far-eastern and the central parts of Turkey. After 1982 the trend analysis results show that main parts of Turkey has a positive trend slope (more wet), but with increasing SPEI time-scale the negative trend slope (more drought) is observed in SEA, EA, and BS. So, before 1982 much wider areas showed negative trend (more drought) than after 1982. Before 1982 the areas that show negative trend used to shrink with increasing SPEI time-scale, while after 1982 these areas get wider with increasing SPEI time-scale.

VCI trend analysis showed that all regions are significant at 0.05 except for a small part in the far northeast of EA, and southern SEA regions, with a positive slope for all regions except for the far northeast of EA region.

The comparison of Mann-Kendell's test results for both SPEI-1, and VCI values shows that they do not coincide, and this is due to the fact that VCI is reflective-based index, while SPEI is Meteorological-based index, so merging two or more indices may resolve such differences.

4.2. Recommendations

This study Highlights the drought trends over all the area of Turkey. The results of the study raise many questions such as, is such a study sufficient? How can we benefit from its results, and what else can be done? What measures to take? In addition, many other questions that lead to several recommendations to know better and be prepared for any results due to the climate change. Taking into consideration that the results of the study show that we are facing not only drought phenomenon, it can be noticed that some areas are getting wetter as well. Following are some recommendations that may be convenient:

- - Further studies and extrapolations for the areas that show a wetter trend to find how wet it is becoming, whether floods are expected in these areas, and the ecological impact of such trends.
- - Performing studies that cover the whole Black Sea region to achieve a clear understanding of the full climatic trends in that area. And whether the trends are more dry or wet.
- - Performing further studies using more drought indices to get better picture of what is going on, including those made by merging two or more indices together such as VegDRI.
- - Further studies to detect the ecological adaptation process to drought and wet trends.
- - Further studies to decide the measures needed to be taken to adapt to drought and wet trends impacts on the country.
- - Further studies that concentrate on the expected drought impact on the main rivers' behavior, and whether worries should be raised to deal with those impacts.
- - Further studies to make a better understanding of what are the most probable causes responsible for the trend changes at the years of change in this study.
- - As the study shows that the situation in the southeastern parts of Turkey is worrying as the drought trend is significant, sever, and persistent, with no signs of regression even after 1981, a further study for this area is needed to fully understand the climatic trends and to assess the necessary measures needed to counter the expected effects of such trend in the future.

REFERENCES

Abiodun, B. J., Salami, A. T., Matthew, O. J., & Odedokun, S. (2013). Potential impacts of afforestation on climate change and extreme events in Nigeria. *Climate Dynamics, 41*(2), 277-293.

Allen, K., Ogden, J., Buckley, B., Cook, E., & Baker, P. (2011). The potential to reconstruct broadscale climate indices associated with southeast Australian droughts from Athrotaxis species, Tasmania. *Climate Dynamics, 37*(9-10), 1799-1821.

Allen, R. G., Pereira, L. S., Raes, D., & Smith, M. (1998). Crop evapotranspiration-Guidelines for computing crop water requirements-FAO Irrigation and drainage paper 56. *Fao, Rome, 300*(9), D05109.

Bajgiran, P. R., Darvishsefat, A. A., Khalili, A., & Makhdoum, M. F. (2008). Using AVHRR-based vegetation indices for drought monitoring in the Northwest of Iran. *Journal of Arid Environments, 72*(6), 1086-1096.

Bayarjargal, Y., Karnieli, A., Bayasgalan, M., Khudulmur, S., Gandush, C., & Tucker, C. (2006). A comparative study of NOAA–AVHRR derived drought indices using change vector analysis. *Remote Sensing of Environment, 105*(1), 9-22.

BEGUERíA, S., Vicente-Serrano, S. M., & Angulo-Martínez, M. (2010). A multiscalar global drought dataset: the SPEIbase: a new gridded product for the analysis of drought variability and impacts. *Bulletin of the American Meteorological Society, 91*(10), 1351-1356.

Beguería, S., Vicente-Serrano, S. M., Reig, F., & Latorre, B. (2014). Standardized precipitation evapotranspiration index (SPEI) revisited: parameter fitting, evapotranspiration models, tools, datasets and drought monitoring. *International Journal of Climatology, 34*(10), 3001-3023.

Benedetti, R., & Rossini, P. (1993). On the use of NDVI profiles as a tool for agricultural statistics: the case study of wheat yield estimate and forecast in Emilia Romagna. *Remote Sensing of Environment, 45*(3), 311-326.

Bhuiyan, C., Singh, R., & Kogan, F. (2006). Monitoring drought dynamics in the Aravalli region (India) using different indices based on ground and remote sensing data. *International Journal of Applied Earth Observation and Geoinformation, 8*(4), 289-302.

Brown, J. F., Wardlow, B. D., Tadesse, T., Hayes, M. J., & Reed, B. C. (2008). The Vegetation Drought Response Index (VegDRI): A new integrated approach for monitoring drought stress in vegetation. *GIScience & Remote Sensing, 45*(1), 16-46.

CGLS, C. G. L. S. Vegetation Condition Index. Retrieved from https://land.copernicus.eu/global/products/vci

CimateDataGuide. (2018). NDVI: Normalized Difference Vegetation Index-3rd generation: NASA/GFSC GIMMS. Retrieved from https://climatedataguide.ucar.edu/climate-data/ndvi-normalized-difference-vegetation-index-3rd-generation-nasagfsc-gimms?qt-climatedatasetmaintabs=2#qt-climatedatasetmaintabs

Doyle Rice, U. T. (2015). California drought cost is 2.7 billion in 2015. Retrieved from https://www.usatoday.com/story/weather/2015/08/19/california-drought-cost-27-billion-2015/32007967/

Gitelson, A. A., Kogan, F., Zakarin, E., Spivak, L., & Lebed, L. (1998). Using AVHRR data for quantitive estimation of vegetation conditions: Calibration and validation. *Advances in Space Research, 22*(5), 673-676.

Hadi, S. J., & Tombul, M. (2018). Long-term spatiotemporal trend analysis of precipitation and temperature over Turkey. *Meteorological Applications, 0*(0). doi:doi:10.1002/met.1712

Hamed, K., & Rao, A. R. (2000). *Flood frequency analysis*: CRC press.

Heim Jr, R. R. (2002). A review of twentieth-century drought indices used in the United States. *Bulletin of the American Meteorological Society, 83*(8), 1149-1165.

Hernandez, E. A., & Uddameri, V. (2014). Standardized precipitation evaporation index (SPEI)-based drought assessment in semi-arid south Texas. *Environmental Earth Sciences, 71*(6), 2491-2501.

Hosking, J. R. (1986). *The theory of probability weighted moments*: IBM Research Division, TJ Watson Research Center.

Kendall, M. G. (1938). A new measure of rank correlation. *Biometrika, 30*(1/2), 81-93.

Kogan, F. N. (1997). Global drought watch from space. *Bulletin of the American Meteorological Society, 78*(4), 621-636.

Kurak geçen kış elektrik fiyatlarında artışa neden olacak. (2018). Retrieved from https://www.haberturk.com/kurak-gecen-kis-elektrik-fiyatlarinda-artisa-neden-olacak-1789971-ekonomi

Li, X., He, B., Quan, X., Liao, Z., & Bai, X. (2015). Use of the standardized precipitation evapotranspiration index (SPEI) to characterize the drying trend in southwest China from 1982–2012. *Remote Sensing, 7*(8), 10917-10937.

Martin-Benito, D., Beeckman, H., & Cañellas, I. (2013). Influence of drought on tree rings and tracheid features of Pinus nigra and Pinus sylvestris in a mesic Mediterranean forest. *European Journal of Forest Research, 132*(1), 33-45.

McKee, T. B., Doesken, N. J., & Kleist, J. (1993). *The relationship of drought frequency and duration to time scales.* Paper presented at the Proceedings of the 8th Conference on Applied Climatology.

Meza, F. J. (2013). Recent trends and ENSO influence on droughts in Northern Chile: An application of the Standardized Precipitation Evapotranspiration Index. *Weather and Climate extremes, 1*, 51-58.

NDMC. (2018a). Types of Drought. Retrieved from http://drought.unl.edu/droughtbasics/typesofdrought.aspx

NDMC. (2018b). Types of Drought Impacts. Retrieved from http://drought.unl.edu/DroughtforKids/HowDoesDroughtAffectOurLives/TypesofDroughtImpacts.aspx

NDMC. (2018c). What is Drought. Retrieved from http://drought.unl.edu/DroughtBasics/WhatisDrought.aspx

Pettitt, A. (1979). A non-parametric approach to the change-point problem. *Applied statistics*, 126-135.

Potop, V. (2011). Evolution of drought severity and its impact on corn in the Republic of Moldova. *Theoretical and Applied Climatology, 105*(3-4), 469-483.

Poyraz, A. Y. (2018). *DROUGHT ANALYSIS USING CORDEX SIMULATIONS OVER THE MEDITERRANEAN CLIMATE REGIONS OF TURKEY.*

Quiring, S. M., & Ganesh, S. (2010). Evaluating the utility of the Vegetation Condition Index (VCI) for monitoring meteorological drought in Texas. *Agricultural and Forest Meteorology, 150*(3), 330-339.

Raleigh, C., Jordan, L., & Salehyan, I. (2008). *Assessing the impact of climate change on migration and conflict.* Paper presented at the paper commissioned by the World

Bank Group for the Social Dimensions of Climate Change workshop, Washington, DC.

sen, P. K. (1968). Estimates of the regression coefficient based on Kendall's tau. *Journal of the American statistical association, 63*(324), 1379-1389.

Sen, Z. (29th July 2015). *Applied Drought Modeling, Prediction, and Mitigation*.

Sensoy, S. (2004). *The mountains influence on Turkey climate.* Paper presented at the Balwois Conference on Water Observation and Information System for Decision Support

Sensoy, S., Demircan, M., Ulupinar, Y., & Balta, İ. (2008). Climate of turkey. *Climate of Turkey. 2007. Devlet Meteoroloji İşleri*.

Singh, R. P., Roy, S., & Kogan, F. (2003). Vegetation and temperature condition indices from NOAA AVHRR data for drought monitoring over India. *International Journal of Remote Sensing, 24*(22), 4393-4402.

Sivakumar, M. V., Stone, R., Sentelhas, P. C., Svoboda, M., Omondi, P., Sarkar, J., & Wardlow, B. (2011). *Agricultural drought indices: Summary and recommendations.* Paper presented at the Agricultural drought indices. Proceedings of the WMO/UNISDR Expert Group Meeting on Agricultural Drought Indices.

Sönmez, F. K., KÖmÜscÜ, A. Ü., Erkan, A., & Turgu, E. (2005). An analysis of spatial and temporal dimension of drought vulnerability in Turkey using the standardized precipitation index. *Natural Hazards, 35*(2), 243-264.

Şorman, A. Ü., Mehr, A. D., & Hadi, S. J. (2018). Study on spatial-temporal variations of Meteorological-Agricultural droughts in Turkey. *Int. Arch. Photogramm. Remote Sens. Spatial Inf. Sci., XLII-3/W4*, 483-490. doi:10.5194/isprs-archives-XLII-3-W4-483-2018

Sruthi, S., & Aslam, M. M. (2015). Agricultural drought analysis using the NDVI and land surface temperature data; a case study of Raichur district. *Aquatic Procedia, 4*, 1258-1264.

Sunar Filiz, C. Ö., Batuhan OSMANOĞLU. (2011). *UZAKTAN ALGILAMA*.

Theil, H. (1950). A rank-invariant method of linear and polynomial regression analysis III, Nederl. Akad. Wet. Proc. 53: 386–392.

Thom, H. C. (1958). A note on the gamma distribution. *Monthly Weather Review, 86*(4), 117-122.

Thornthwaite, C. W. (1948). An approach toward a rational classification of climate. *Geographical review, 38*(1), 55-94.

Tucker, C. J., Pinzon, J. E., Brown, M. E., Slayback, D. A., Pak, E. W., Mahoney, R., . . . El Saleous, N. (2005). An extended AVHRR 8-km NDVI dataset compatible with MODIS and SPOT vegetation NDVI data. *International Journal of Remote Sensing, 26*(20), 4485-4498.

Türkeş, M., & Tatlı, H. (2009). Use of the standardized precipitation index (SPI) and a modified SPI for shaping the drought probabilities over Turkey. *International Journal of Climatology, 29*(15), 2270-2282.

Türkeş, M., Yozgatlıgil, C., Batmaz, İ., İyigün, C., Koç, E. K., Fahmi, F. M., & Aslan, S. (2016). Has the climate been changing in Turkey? Regional climate change signals based on a comparative statistical analysis of two consecutive time periods, 1950-1980 and 1981-2010. *Climate Research, 70*(1), 77-93.

Unal, Y. S., Deniz, A., Toros, H., & Incecik, S. (2012). Temporal and spatial patterns of precipitation variability for annual, wet, and dry seasons in Turkey. *International Journal of Climatology, 32*(3), 392-405.

Unganai, L. S., & Kogan, F. N. (1998). Drought monitoring and corn yield estimation in Southern Africa from AVHRR data. *Remote Sensing of Environment, 63*(3), 219-232.

Vicente-Serrano, S. M. About the SPEI Drought monitoring and analysis based on climatic indices. Retrieved from http://spei.csic.es/home.html

Vicente-Serrano, S. M. (2007). Evaluating the impact of drought using remote sensing in a Mediterranean, semi-arid region. *Natural Hazards, 40*(1), 173-208.

Vicente-Serrano, S. M., Beguería, S., & López-Moreno, J. I. (2010). A multiscalar drought index sensitive to global warming: the standardized precipitation evapotranspiration index. *Journal of climate, 23*(7), 1696-1718.

Wang, W., Zhu, Y., Xu, R., & Liu, J. (2015). Drought severity change in China during 1961–2012 indicated by SPI and SPEI. *Natural Hazards, 75*(3), 2437-2451.

WMO. (2012). *Standardized Precipitation Index User Guide*: World Meteorological Organization.

WMO. (2016). *Handbook of Drought Indicators and Indices*: World Meteorological Organization